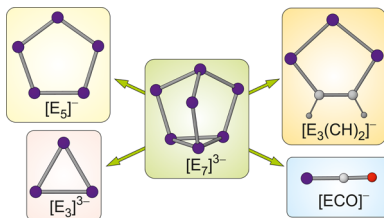


From Clusters to Unorthodox Pnictogen Sources: Solution-Phase Reactivity of $[E_7]^{3-}$ ($E = P-Sb$) Anions*

Robert S. P. Turbervill and Jose M. Goicoechea*

Department of Chemistry, Chemistry Research Laboratory, University of Oxford, 12 Mansfield Road, Oxford OX1 3TA, United Kingdom



CONTENTS

1. Introduction	10807
2. Relationship between Solid-State Phases and the Chemistry of Polyphosphides in Solution	10807
2.1. Historical Perspective	10807
2.2. Polyphosphides	10808
2.3. Common Polyphosphides and Their Redox Chemistry	10809
3. Synthesis and Structure of $[E_7]^{3-}$ Clusters	10811
4. Brønsted Acid–Base Chemistry and Isomerism of $[H_nE]^{(3-n)-}$ Clusters	10812
4.1. $[HE_7]^{2-}$	10813
4.2. $[H_2E_7]^-$	10813
4.3. $[H_3E_7]$	10813
4.4. Isomerism in $[E_7R_n]^{(3-n)-}$ Clusters	10813
4.4.1. $[E_7R_1]^-$	10813
4.4.2. $[E_7R_2]^-$	10814
4.4.3. $[E_7R_3]$	10814
5. Reactivity of $[E_7]^{3-}$ toward Nonmetal Main-Group Electrophiles and $FeCp(CO)_2$	10814
5.1. Salt Elimination Reactions	10814
5.2. Hydropnictination Reactions	10815
6. Coordination Chemistry	10816
6.1. Review of Bonding Modes	10816
6.2. Structure and Bonding	10816
6.2.1. η^2 Coordination Mode	10816
6.2.2. Dinuclear Bridged Clusters	10817
6.2.3. η^4 Coordination Mode	10819
7. Cluster Fragmentation and Rearrangement	10821
7.1. Metal-Mediated Activation	10821
7.2. Activation by Unsaturated Organic Substrates	10823
8. Conclusion	10824
Author Information	10824
Corresponding Author	10824
Author Contributions	10824
Notes	10824
Biographies	10824
Acknowledgments	10825
Abbreviations	10825
References	10825

1. INTRODUCTION

The controlled chemical activation of white phosphorus (P_4) is a versatile, albeit often unpredictable, route to phosphorus-containing species of varied nuclearities. This area of chemistry has historically received significant attention as direct activation of white phosphorus by transition-metal and main-group complexes represents a useful way of circumventing the use of toxic PCl_3 as a feedstock. Consequently, this research area has been extensively reviewed in the chemical literature.^{1–10}

However, it is worth noting that use of white phosphorus as a precursor is not without its pitfalls on account of its toxicity and highly pyrophoric nature.

In principle, many of the same transformations available for P_4 are also possible employing other closely related cage compounds, such as the bare group 15 Zintl anion $[P_7]^{3-}$; however, this area of research remains largely underexplored (the heptaphosphide trianion can be thought of as a P_4 molecule in which three phosphide vertices, P^- , are inserted into adjacent P–P bonds). The chemistry of $[E_7]^{3-}$ ($E = P, As$) cages has previously been reviewed on two occasions in the context of the greater chemistry of the Zintl ions of groups 14 and 15.^{11,12} In treating the topic of $[E_7]^{3-}$ clusters, these reviews largely focus on their coordination chemistry and on the heteroatomic metal clusters available for the heavier group 15 elements such as As, Sb, and Bi. However, the redox chemistry and Brønsted basicity of these species (and their relationship with hydrogenpolyphosphides) remain largely undersurveyed. Moreover, little attention has been paid to chemical activation of the lighter cages ($[P_7]^{3-}$ and $[As_7]^{3-}$) to yield species with nuclearities other than those of the parent clusters. These latter patterns of reactivity will form the focus of our review. A pictorial summary of selected transformations covered in this review article is provided in Figure 1, paying particular attention to recent discoveries which show that $[P_7]^{3-}$ and $[As_7]^{3-}$ may be used as sources of pnictide (E^-) and polypnictide (E_n^-) moieties.

2. RELATIONSHIP BETWEEN SOLID-STATE PHASES AND THE CHEMISTRY OF POLYPHOSPHIDES IN SOLUTION

2.1. Historical Perspective

The first steps in Zintl anion chemistry were taken by Joannis in 1891, who observed that elemental lead could be dissolved into liquid ammonia solutions of sodium, giving rise to intensely colored, green solutions.¹³ He later showed that

Received: July 18, 2014

Published: October 21, 2014

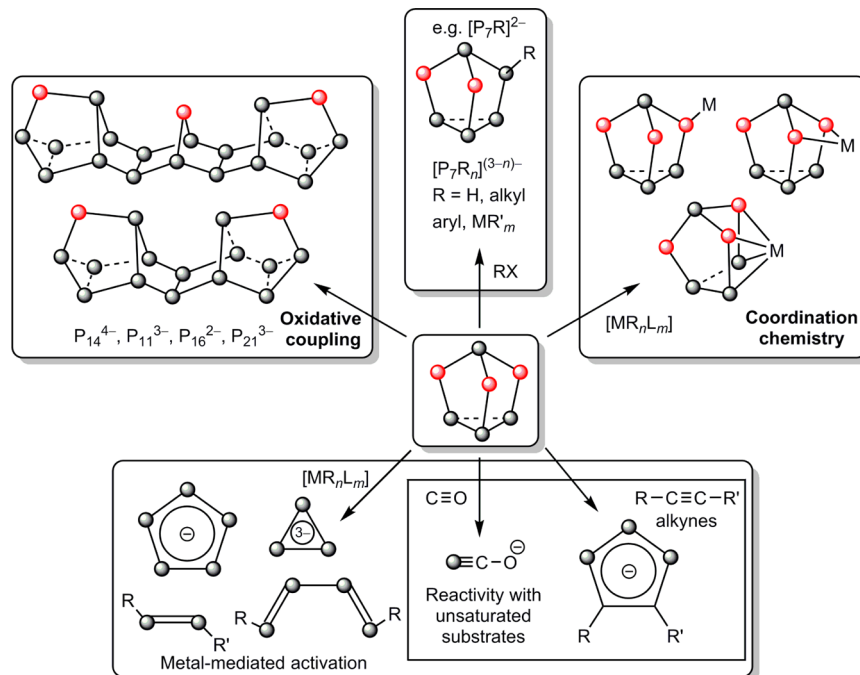


Figure 1. Selected reactions of $[E_7]^{3-}$ clusters. Atoms bearing a formal negative charge are highlighted in red. $[MR_nL_m]$ represents metal complexes.

antimony gives rise to yellow solutions under the same conditions,^{14,15} while Kraus expanded the work to tin.¹⁶ The approximate stoichiometries of the solutions were determined by Smyth and Peck (2.24 atoms of Pb per Na atom and 2.33 atoms of Sb per Na atom, respectively).^{17,18} However, it was not until 1931 that the identities of the anions responsible for the coloration were determined. Eduard Zintl, for whom the so-called Zintl anions would later be named, identified the $[Pb_9]^{4-}$, $[Sn_9]^{4-}$, $[Sb_7]^{3-}$, and $[As_7]^{3-}$ anions present in liquid ammonia solutions by potentiometric titration.^{19–22}

Zintl phases, intermetallic alloys formed by the high-temperature reaction of s-block metals with p-block elements, contain polyatomic p-block anions. In some cases, these are cluster anions, either the same as, or related to those observed in solution by Zintl. In 1970, Kummer and Diehl demonstrated that dissolution of the alloy Na_4Sn_9 into ethylenediamine resulted in formation of the same $[Sn_9]^{4-}$ homoatomic polyanion observed by Zintl and Joannis.²³ Further advances were made when the work of Corbett and co-workers showed that addition of cation sequestering agents, in particular the crypt and 2,2,2-crypt, stabilized the resulting solutions and also allowed crystallization of the compounds for structural characterization.²⁴ This route, namely, dissolution of precursor Zintl phases into polar, aprotic solvents (such as ammonia, ethylenediamine, pyridine, or DMF), typically in the presence of a cation sequestering agent (cryptands or crown ethers), has proved to be the most convenient way to generate stable solutions of the Zintl cluster anions for further study. Initially this permitted the crystallization of $[K(2,2,2\text{-crypt})_3][Sb_7]$,²⁵ but the methodology was later extended to other Zintl phases, allowing for the characterization of a wealth of both homoatomic and heteroatomic polyanions.^{26,27}

2.2. Polyphosphides

The rich chain and cage chemistry of polyphosphanes and polyphosphides has been extensively studied and reviewed, primarily by the groups of Baudler and von Schnerring.^{28–31}

There are two principal routes that have been taken for their synthesis: (1) direct combination of an alkali metal with elemental phosphorus either in solution or the solid state or (2) reaction of phosphanes with elemental phosphorus under reducing or basic conditions. Depending on the exact reaction conditions and stoichiometries used, a plethora of unique polyphosphides can be synthesized, either as binary solids or as solvated molecular systems.

Synthesis of polyphosphides by reaction of white phosphorus with alkali metals in ammonia can be considered a reductive activation of the P_4 cage. It seems reasonable to assume that the first step is a one- or two-electron transfer, leading to formation of an anionic or a dianionic P_4 moiety. These species have yet to be isolated, but Baudler and co-workers reported the synthesis of $[HP_4]^-$, the first isolable reduction product, by reaction of P_4 with K/naphthalene in DME.³² This species is only stable at low temperature, decomposing to higher polyphosphides on warming. The $[HP_4]^-$ anion is in all likelihood a precursor for the more aggregated polyphosphides. Using this reductive methodology a wide range of polyphosphides can be synthesized and characterized. Frequently it is not possible to achieve isolation of a single product, but instead a mixture of polyphosphides is obtained that can be enriched in a particular species (e.g., $[P_{19}]^{3-}$) by careful tuning of reaction conditions.³³ The product distribution is particularly dependent on stoichiometry, temperature, and solvent. Low boiling point, highly polar solvents such as ammonia tend to favor formation of relatively small polyphosphides, whereas higher boiling or less polar solvents tend to favor formation of more highly aggregated anions.

Binary solids and molecular anions are inextricably linked by both shared structural motifs and indeed the ability to extract solvated anions from the solid phases themselves. The known homoatomic group 15 polypnictide containing phases are highlighted in Tables 1 and 2, specifically those that can be isolated and characterized using both solution and solid-state methods.

Table 1. Isolated Homoatomic Chain, Ring, and Cage Structural Motifs Found in Polypnictides Synthesized through Solid-State Methods

anion	element	compound	ref
[E ₂] ²⁻	Bi	A ₃ Bi ₂ (A = K, Rb, Cs)	34
[E ₃] ³⁻	As	Cs ₃ As ₃	35
[E ₄] ⁴⁻	As, Sb, Bi	A ₅ E ₄ (A = K, Rb, Cs)	36
[E ₅] ⁵⁻	As	ABA ₂ As ₅ (A = K, Rb)	37
[E ₆] ⁴⁻	P	K ₄ P ₆	38
		Rb ₄ P ₆	39, 40
		Cs ₄ P ₆	39
[E ₇] ³⁻	As	A ₄ As ₆ (A = Rb, Cs)	41
	P	Li ₃ P ₇	42
		A ₃ P ₇ (A = Na, K, Rb)	43
		Cs ₃ P ₇	43, 44
	As	Ae ₃ [P ₇] ₂ (Ae = Sr, Ba)	45, 46
		Li ₃ As ₇	47
		Na ₃ As ₇	48
		A ₃ As ₇ (A = K, Cs)	35
	Sb	Rb ₃ As ₇	35, 49
		Ba ₃ [As ₇] ₂	50
[E ₁₁] ³⁻	P	Rb ₃ Sb ₇	51
		Cs ₃ Sb ₇	51, 52
	As	Na ₃ P ₁₁	53, 54
		A ₃ P ₁₁ (A = K, Rb, Cs)	54
		K ₃ As ₁₁	54
		A ₃ As ₁₁ (A = Rb, Cs)	54, 55

2.3. Common Polyphosphides and Their Redox Chemistry

Of the clusters highlighted, only [E₇]³⁻ and [E₁₁]³⁻ (E = P, As, Sb) can be isolated from solution and using solid-state methods. Of these two, [P₇]³⁻ has been the most extensively studied on account of its synthetic accessibility and well-understood behavior in both solution and the solid state.

In addition to the reductive routes discussed above, formation of higher nuclearity polyphosphides from mild oxidative coupling of [P₇]³⁻ is frequently observed. As such, it becomes useful to define an “average reduction state” of the anion simply by dividing the overall cluster charge by the number of phosphorus atoms. It is important to note that these numbers should not necessarily be taken as indicative of any charge delocalization throughout these anions, although quantum chemical calculations demonstrate that significant delocalization is known to occur. From a valence perspective, formally such cluster anions possess isolated anionic charges on the two-coordinate phosphorus atoms. The obvious exception to this is the *cyclo*-[P₅]⁻ anion, isolobal to *cyclo*-[C₅H₅]⁻, which has a single negative charge delocalized throughout the aromatic system. We will briefly discuss these systems as a function of their average reduction state or average negative charge per P atom. The chemistry of the polyarsenide, polystibide, and polybismuthide analogues is substantially less well developed, no doubt due to the lack of a suitable spectroscopic handle with which to monitor reactions.

Hypothetical dimerization (or oxidative coupling) of two [P₇]³⁻ cages by formation of a single bond between two bridging atoms gives rise to the [P₁₄]⁴⁻ anion (Table 3). Although the cage geometry is clearly related to that of [P₇]³⁻, the known synthetic routes do not start from this anion. Instead, it is formed by reaction of lithium with white phosphorus in liquid ammonia or sodium with red phosphorus in ethylenediamine in the appropriate stoichiometric ratio.^{98,99}

The structure reveals the linking of two nortricyclane-like P₇ cages in an “up–down” fashion to form the polyphosphide [P₁₄]⁴⁻. No definitive ³¹P NMR data exists for this anion. Miluykov, Hey-Hawkins and co-workers reported variable-temperature ³¹P NMR studies on the sodium salt, although the published spectra appear to be a mixture of [P₂₁]³⁻ and [HP₇]²⁻ (*vide infra*). It is likely that the anion is not stable due to the relatively high average charge per phosphorus atom and the absence of a fluxional mechanism which allows for delocalization of 4– negative charge over all of the cluster atoms. Without invoking more complex dissociative mechanisms, the [P₁₄]⁴⁻ cage can only delocalize its 4– charge over eight vertices (giving it a net –0.5 charge for these particular atoms). In addition, loss of 3D aromaticity also accounts for the fact that, despite having a smaller net charge per P atom, the [P₁₄]⁴⁻ cage is notably less stable than [P₇]³⁻.

The slightly oxidized [P₁₁]³⁻ anion is accessible through both solid-state- and solution-based methods.^{53,54,75,88–92} The 11-vertex trianion can be extracted into solution by dissolution of preformed phases such as Cs₃P₁₁ and subsequently recrystallized as alkali metal or tetraalkylammonium salts.^{75,88–92} The MAS ³¹P NMR spectrum of this anion has been reported and features four resonances at 174.5, 167.9, –102.3, and –209.4 ppm which integrate in a 3:3:2:3 ratio (with significant overlap of the two lower field resonances). On account of its high basicity, the protonated [HP₁₁]²⁻ cage is also known. Oxidative coupling of two [P₁₁]³⁻ cages affords the dimeric anion [P₂₂]⁴⁻.¹⁰³ To our knowledge, this anion has yet to be isolated from solutions of [P₇]³⁻.

The first report of the free pentaphosphacyclopentadienide (or pentaphospholide) anion was in 1987 by the group of Baudler, who reported its formation among other polyphosphides and phospholides on reaction of P₄ with sodium in diglyme.⁶⁵ This synthesis was further refined to give pure (by ³¹P NMR spectroscopy) solutions of [Na(18-crown-6)][P₅] in THF.^{66,67} These solutions were reported to be extremely air and moisture sensitive and decompose to [P₁₆]²⁻ and [P₂₁]³⁻ on attempts to isolate. The anion displays a singlet resonance at around 470 ppm, suggesting a single phosphorus environment in a highly deshielded, aromatic system.

Coupling of three seven-vertex cages gives rise to the [P₂₁]³⁻ anion. The published synthetic route involves reduction of white phosphorus with substoichiometric sodium in DME,¹⁰² although it is frequently observed in [P₇]³⁻ chemistry through mild cage oxidation processes. The anion possesses an extremely characteristic room-temperature ³¹P NMR spectrum with resonances at 72, 61, –15, –108, –118, –146, and –169 ppm integrating in the ratio 2:8:2:1:2:2:4.

The most oxidized polyphosphide commonly observed in [P₇]³⁻ chemistry before the ultimate oxidation to elemental phosphorus is [P₁₆]²⁻. This consists of two P₇ fragments linked in an “up–up” fashion by a P₂ unit (Table 3). In contrast to [P₁₄]⁴⁻ and [P₂₁]³⁻, this was first prepared by reaction of P₄ with LiPH₂ or oxidation of [P₇]³⁻ with [PPh₄][Cl].¹⁰⁰ Baudler and co-workers later reported the synthesis via disproportionation of Li₂[HP₇].^{106,107} The ³¹P NMR spectrum shows resonances at 60, 38, 6, –34, –134, and –180 ppm integrating in the ratio 2:1:1:1:1:2.

Redox interconversion of [P₁₆]²⁻ and [P₂₁]³⁻ has been reported by Guerin and Richeson.¹⁰⁸ Upon dissolving a pure sample of K₂P₁₆ in THF, ³¹P NMR and X-ray fluorescence measurements showed conversion to [P₂₁]³⁻ and elemental phosphorus. Removing the THF from such solutions and

Table 2. Isolated Homoatomic Chain, Ring, and Cage Structural Motifs Found in Polypnictides Synthesized through Solution Methods (and in some cases also solid-state methods)^a

anion	element	compound	ref	synthetic method
[E ₂] ²⁻	Bi	[K(2,2,2-crypt)] ₂ [Bi ₂]	56	solution/solid state
[E ₄] ²⁻	P	Cs ₂ [P ₄]·2NH ₃	57, 58	solution
		[K(18-crown-6)] ₂ [P ₄]·2NH ₃	59	solution
	As	[K(18-crown-6)] ₂ [As ₄]	59	solution
		[Li(NH ₃) ₄] ₂ [As ₄]	60	solution
		[Na(NH ₃) ₅] ₂ [As ₄]·3NH ₃	60	solution
		[Cs _{0.35} Rb _{0.65} (2,2,2-crypt)] ₂ [As ₄]·2NH ₃	60	solution
	Sb	[K(2,2,2-crypt)] ₂ [Sb ₄]	61	solution
	Bi	[K(2,2,2-crypt)] ₂ [Bi ₄]	62	solution
		[A(2,2,2-crypt)] ₂ [Bi ₄] (A = K, Rb)	62, 63	solution
[E ₄] ⁶⁻	Bi	K ₆ [Bi ₄]·8NH ₃	64	solution
[E ₅] ⁻	P	NaP ₅ solutions in THF	65–67	solution
[E ₅] ⁵⁻	Sb	[Li(NH ₃) ₄] ₃ [Li(NH ₃) ₂][Sb ₅]·2NH ₃	68	solution
[E ₆] ⁴⁻	As	[Rb(18-crown-6)] ₂ Rb ₂ As ₆ ·6NH ₃	69	solution/solid state
[E ₇] ³⁻	P	[Li(TMEDA)] ₃ [P ₇]	70	solution/solid state
		Cs ₃ [P ₇]·3NH ₃	71	solution/solid state
		Rb ₃ [P ₇]·7NH ₃	58	solution/solid state
		Ba ₃ [P ₇] ₂ ·18NH ₃	72	solution/solid state
		[NEt ₃ Me]Cs ₂ [P ₇]·NH ₃	73	solution/solid state
		[NEt ₄]Cs ₂ [P ₇]·4NH ₃	73	solution/solid state
		[NEtMe ₃]Cs ₂ [P ₇]·2NH ₃	74	solution/solid state
		[NMe ₄] ₂ Rb[P ₇]·NH ₃	75	solution/solid state
		[Rb(18-crown-6)] ₃ [P ₇]·6NH ₃	58	solution/solid state
		K ₃ [K(18-crown-6)] ₃ [P ₇] ₂ ·10NH ₃	58	solution/solid state
	As	[Li(TMEDA)] ₃ [As ₇]·1.5toluene	76	solution/solid state
		[Li(NH ₃) ₄] ₃ [As ₇]·NH ₃	77	solution/solid state
		Cs ₃ [As ₇]·6NH ₃	77	solution/solid state
		Cs ₃ [As ₇]·NH ₃	78	solution/solid state
		[Li(TMEDA)] ₃ [As ₇]·OEt ₂	79	solution/solid state
		[Li(DME)] ₃ [As ₇]·OEt ₂	80	solution/solid state
		[NMe ₄] ₂ Rb[As ₇]·NH ₃	81	solution/solid state
		[Rb(18-crown-6)] ₃ [As ₇]·8NH ₃	77	solution/solid state
		[PPh ₄] ₂ Cs[As ₇]·5NH ₃	77	solution/solid state
		K ₃ [K(2,2,2-crypt)] ₃ [As ₇] ₂	82	solution/solid state
	Sb	[Li(TMEDA)] ₃ [Sb ₇]·toluene	83	solution/solid state
		[Na(2,2,2-crypt)] ₃ [Sb ₇]	25	solution/solid state
		Na ₃ [Sb ₇]·4en	84	solution/solid state
		[Na(TMEDA)] ₃ [Sb ₇]·3THF	76	solution/solid state
		[Li(NHMe ₂) ₂] ₃ [Sb ₇]	83	solution/solid state
		[Li(TMEDA)] ₃ [Sb ₇]·3tol	83	solution/solid state
		[K(2,2,2-crypt)] ₃ [Sb ₇]·2en	61	solution/solid state
		[Na(PMDETA)] ₃ [Sb ₇]·toluene	85	solution/solid state
		[Rb(18-crown-6)] ₃ [Sb ₇]·4NH ₃	86	solution/solid state
[E ₈] ⁸⁻	Sb	[K ₁₇ (Sb ₈) ₂ (NH ₂) ₂]·17.5NH ₃	87	solution
[E ₁₁] ³⁻	P	[NMe ₃] ₃ [P ₁₁]	88	solution/solid state
		Cs ₃ [P ₁₁]·3NH ₃	89	solution/solid state
		BaCs[P ₁₁]·NH ₃	90	solution/solid state
		Cs[NEt ₃ Me] ₂ [P ₁₁]·5NH ₃	91	solution/solid state
		Cs ₂ [NEt ₄][P ₁₁]	75	solution/solid state
		[K(18-crown-6)] ₃ [P ₁₁]·2en	92	solution/solid state
	As	[K(2,2,2-crypt)] ₃ [As ₁₁]	93	solution/solid state
	Sb	[Na(2,2,2-crypt)] ₃ [Sb ₁₁]	94	solution
		[K(18-crown-6)(NH ₃) ₂] ₂ [Sb ₁₁]·5.5NH ₃	93	solution
		[K(2,2,2-crypt)] ₃ [Sb ₁₁]	95	solution
		[Li(12-crown-4) ₂] ₃ [Sb ₁₁]	96	solution
	Bi	[K(2,2,2-crypt)] ₃ [Bi ₁₁]·2py·tol	97	solution
[E ₁₄] ⁴⁻	P	Na ₄ (DME) _{7.5} [P ₁₄]	98	solution
		[Na(en) _{1.5}] ₄ [P ₁₄]	98	solution
		[Li(NH ₃) ₄] ₄ [P ₁₄]·NH ₃	99	solution
	As	[Rb(18-crown-6)] ₄ [As ₁₄]·6NH ₃	99	solution

Table 2. continued

anion	element	compound	ref	synthetic method
[E ₁₆] ²⁻	P	[Na(18-crown-6)] ₂ [18-crown-6][P ₁₆] [PPh ₄] ₂ [P ₁₆]	100 101	solution solution
[E ₁₉] ³⁻	P	Li, Na, K in DMF, THF or DME	33	solution
[E ₂₁] ³⁻	P	Li or Na ₃ P ₂₁ solutions	102	solution
[E ₂₂] ⁴⁻	P	[NETMe ₃] ₄ [P ₂₂]·2NH ₃	103	solution
	As	[Rb(2,2,2-crypt)] ₄ [As ₂₂]·4DMF	104	solution
[E ₂₆] ⁴⁻	P	Li ₄ P ₂₆ ·16THF	105	solution

^aIn some cases structures are known with many different cations or solvates. We endeavored to include all of these.

Table 3. Summary of Structure, ³¹P NMR Data, and Average Charge Per P Atom for Polyphosphides Commonly Observed in the Chemistry of [P₇]³⁻

Structure	[P ₇] ³⁻	[P ₁₄] ⁴⁻	[P ₁₁] ³⁻
³¹ P NMR (ppm)	-119 at 20°C	-	174.5, 167.9, -102.3, -209.4
Charge per P atom	-0.429	-0.286	-0.273
Structure	[P ₅] ⁻	[P ₂₁] ³⁻	[P ₁₆] ²⁻
³¹ P NMR (ppm)	470	72, 61, -15, -108, -118, -146, -169	60, 38, 6, -34, -134, -180
Charge per P atom	-0.200	-0.143	-0.125

redissolving the residue in ethanol restored the ³¹P NMR spectrum of [P₁₆]²⁻. This facile interconversion process is evidence for the shallow energy surface on which such species lie. It appears that the most stable solution polyphosphides are those where either the negative charges are well separated (such as in [P₂₁]³⁻ and [P₁₆]²⁻) or a mechanism exists for transfer of charge over multiple phosphorus atoms (fluxional processes in [P₇]³⁻ or delocalization in [P₅]⁻). It is interesting to note that conversion between [P₂₁]³⁻ and [P₁₆]²⁻ would formally involve a [P₅]⁻ moiety, although spectroscopic studies of such mixtures are invariably more complex.

One-electron oxidation of an [E₇]³⁻ cluster should result in a putative [E₇]²⁻ radical anion cage. This might be expected to dimerize into an [E₁₄]⁴⁻ anion, discussed above. Examples are not known for either phosphorus or antimony, but recently, Weiss, Khanna, Sen, and co-workers reported the synthesis and isolation of a compound that is formulated as [As₇]²⁻.¹⁰⁹ Observation of a signal in the ESR spectrum and an apparently reversible [As₇]³⁻/[As₇]²⁻ redox couple is recorded; however, crystal structure determination is inconclusive. Computational studies of the [As₇]²⁻ anion demonstrate that such a species should have a significantly different geometry to that of [As₇]³⁻ (a result of a Jahn–Teller distortion); however, comparison with the structure obtained from single-crystal X-ray diffraction studies is not possible due to extensive positional disorder in

the latter. This makes it challenging to conclusively exclude the possibility that the protonated [HAs₇]²⁻ anion has not been formed, contaminated by a small amount of a paramagnetic impurity.

It is also worth noting at this stage that heteroatomic clusters of the type [P_(7-n)As_n]³⁻ have also been reported by dissolution of ternary phases containing both phosphorus and arsenic.¹¹⁰ It is possible that controlled oxidation of such species may be used to access heteroatomic analogues of the aforementioned polyphosphides.

3. SYNTHESIS AND STRUCTURE OF [E₇]³⁻ CLUSTERS

There are two major classes of Zintl phases that contain the [E₇]³⁻ polyanion. The A₃E₇ (A = Li, Na, K, Rb, Cs; E = P, As, Sb) phases are formed with group 1 metals,^{35,42–44,47,48,51,52} and the Ae₃E₁₄ (Ae = Sr, Ba; E = P, As) phases are formed with group 2 metals.^{45,46,50} In both cases, the crystal structures of the known phases contain discrete [E₇]³⁻ units linked into a three-dimensional lattice by interspersed metal cations. The alkali-metal-containing phases are more frequently used as the contemporary solution sources of [E₇]³⁻, in particular, the K₃E₇ phase. This is mainly attributable to the reduced cost of K⁺ sequestering agents 2,2,2-crypt and 18-crown-6 relative to those specific for the other alkali metals.

There are other reported synthetic methods to the $[E_7]^{3-}$ anions that do not require solid-state chemistry and are instead entirely solution based. The most commonly cited source of $[P_7]^{3-}$ is $[Li(DME)]_3[P_7]$. This is synthesized by nucleophilic cleavage of P_4 with $LiPH_2$ in dimethoxyethane.¹¹¹ Requiring the use of both phosphane and white phosphorus, it is unsurprising that more recent work has largely used the Zintl phases as a starting material. More amenable solution-based strategies for synthesis of $[P_7]^{3-}$ are also available which require the use of red phosphorus and thus significantly reduce the risk associated with manipulation of pyrophoric precursors.^{112,113} An analogous route does not exist for the heavier congeners $[As_7]^{3-}$ and $[Sb_7]^{3-}$; however, an alternative method involving thermolysis of heterobimetallic molecules has been detailed by Wright and co-workers.^{83,96}

Polyatomic anions of group 15 are electron precise, and their bonding can be described using the simple two-center, two-electron bonding model. In the solid state, the $[E_7]^{3-}$ cluster anion adopts a C_{3v} -symmetric nortricyclane-like structure (Figure 2). The basal three-membered ring (E5, E6, E7) is

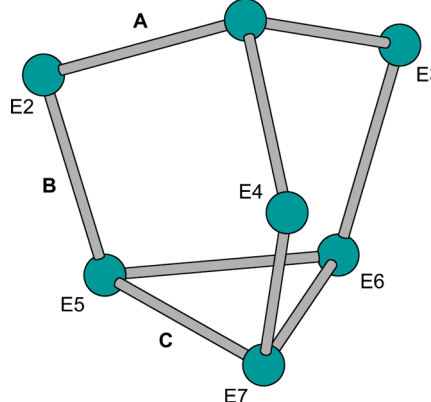


Figure 2. Structure of the $[E_7]^{3-}$ anion ($E = P, As, Sb$) with atoms and unique bonds labeled.

linked by three bridging atoms (E2, E3, E4) to a single apical atom (E1). Each of the bridging atoms can be considered as being a pseudogroup 16 atom, thus carrying a formal negative charge, in agreement with the overall three minus charge of the anion.¹¹⁴

Analysis of the interatomic distances shows that the longest bonds are found in the base of the clusters (Table 4). The basal

Table 4. Mean Bond Lengths in the $[E_7]^{3-}$ Clusters^a

bond	mean length in $[P_7]^{3-}$ (Å)	mean length in $[As_7]^{3-}$ (Å)	mean length in $[Sb_7]^{3-}$ (Å)
A	2.204	2.432	2.78
B	2.150	2.399	2.70
C	2.255	2.498	2.86

^aLabeling refers to that used in Figure 2.

P–P interatomic distances of 2.255(av) Å and P–P–P angles of approximately 60° in $[Li(TMEDA)]_3[P_7]$ are very similar to those observed for white phosphorus (2.21 Å; 60.0°).¹¹⁵ As would be expected, the arsenic and antimony congeners possess structures that are identical, albeit with substantially lengthened bonds.^{25,35,47–52,61,76–86}

The structure and dynamics of the $[P_7]^{3-}$ cluster have been extensively probed using ^{31}P NMR spectroscopy, both in solution and in the solid-state. At room temperature, in solution, only a very broad, nondistinct resonance is observed (the reader is referred to p 498 of ref 28 for representative NMR spectra).²⁸ On heating to 50 °C this sharpens to a singlet at –119 ppm, implying the equivalence of all seven atoms on the NMR time scale via a fluxional process that exchanges them all. Upon cooling to –60 °C this fluxionality is frozen out, and the spectrum reveals three multiplet resonances at –57, –103, and –162 ppm integrating in the ratio 1:3:3. These were assigned to the apical vertex, bridging vertices, and basal vertices, respectively. Similar behavior is observed in variable-temperature solid-state ^{31}P NMR spectroscopy on amorphous samples of $[Li(DME)]_3[P_7]$.¹¹⁶ This has been attributed to a reversible valence tautomerism process analogous to the degenerate Cope rearrangement in the hydrocarbon bullvalene (Figure 3), although with clear differences.^{117–120} The process

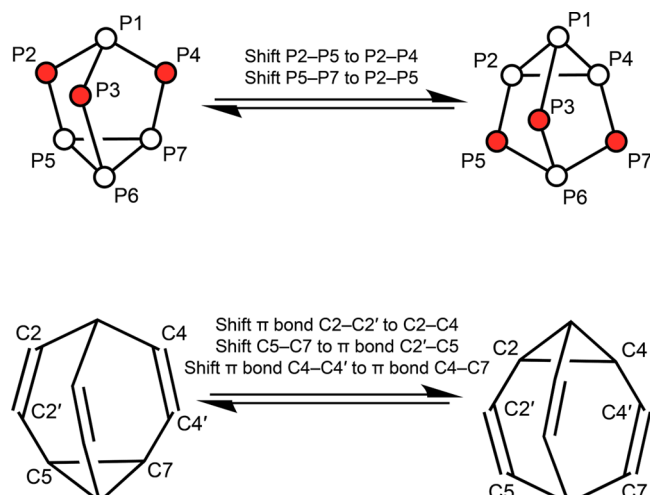


Figure 3. Valence tautomerism processes occurring in $[P_7]^{3-}$ (top) and the hydrocarbon bullvalene (bottom). Atoms bearing a formal negative charge are highlighted in red. Only one such interconversion is shown; for $[P_7]^{3-}$ there are $7!/3 = 1680$ valence tautomeric forms, and for bullvalene there are $10!/3 = 1\,209\,600$.

is undoubtedly driven by the strain inherent within the base of the cluster and assisted by the presence of easily movable electron pairs on the bridging phosphide vertices (and electron delocalization throughout the cluster). It seems reasonable to assume that there are analogous dynamic processes in the $[As_7]^{3-}$ and $[Sb_7]^{3-}$ clusters, although neither element has a suitable NMR active nucleus that would allow for this phenomenon to be investigated.

4. BRØNSTED ACID–BASE CHEMISTRY AND ISOMERISM OF $[H_nE_7]^{(3-n)-}$ CLUSTERS

Of all the elements, only carbon has more known hydrides than phosphorus (which is in no doubt a result of the diagonal relationship between these two elements).³⁰ Individual polyphosphanes (H_nP_m) can be detected by their mass spectra, but more detailed analysis of their structures, particularly for the complex polyphosphorus cages found in hydrogen-poor phosphanes, can only be determined by a combination of ^{31}P NMR spectroscopy and diffraction methods.²⁸ Due to their low solubility and tendency to form amorphous solids or liquids,

many of the known polyphosphanes are not well characterized. Polyphosphides, however, are well explored and frequently structurally related to the parent polyphosphanes.^{29,31} Despite the sole difference between the two series being the loss or gain of protons through Brønsted acid–base chemistry, this concept is not well explored experimentally. Synthesis of these compounds is not as simple as the above thought experiment might suggest, however. There is a marked tendency for disproportionation upon protonation of polyphosphides, resulting in formation of higher polyphosphide species and phosphane, PH₃. As such, there are a dearth of intermediate hydrogen polyphosphides bridging the gap between polyphosphides and polyphosphanes. One exception to this are those derived from the [P₇]³⁻ Zintl anion, forming the homologous series [HP₇]²⁻, [H₂P₇]⁻, and [H₃P₇] upon sequential protonation. As the simplest conceivable substituted heptaphosphite clusters, these also serve as an excellent demonstration of the types of isomerism possible in the substituted clusters.

4.1. [HE₇]²⁻

The hydrogenheptaphosphide anion, [HP₇]²⁻, was first identified by Baudler and co-workers in solution in 1984 by the disproportionation reaction of diphosphane with ⁷BuLi at low temperature.¹²¹ At room temperature the cage atoms undergo an exchange process that renders two sets of them equivalent on the NMR time scale in a manner analogous to the parent [P₇]³⁻ cage (Figure 4). On cooling to –60 °C the

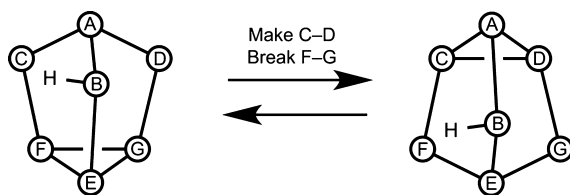


Figure 4. Ball and stick diagram showing the interconversion fluxional process within [HP₇]²⁻. See section 4.4.1 for a full discussion of the isomerism occurring in [E₇R]²⁻-type clusters.

fluxional process is frozen out, with seven resonances corresponding to the seven inequivalent phosphorus environments being observed at –9.0, –67.5, –83.7, –119.4, –134.8, –145.2, and –215.9 ppm (see section 4.4.1).

It was not until 2004 that the anion was isolated and an X-ray structural study performed, confirming the connectivity of the anion proposed by Baudler. Aschenbrenner and Korber synthesized [PPh₄]₂[HP₇]·3NH₃ through reaction of K₃P₇, Amberlyst 15 proton exchange resin, and [PPh₄][Br] in liquid ammonia.¹²² Further crystal structures were reported for the [K(18-crown-6)]⁺, [K(2,2,2-crypt)]⁺, and [K(dibenzo-18-crown-6)]⁺ salts in 2006.¹²³

As part of our recent investigations into the reactivity of heptaphosphide cages, we recently reported a facile high-yielding synthesis of the [HP₇]²⁻ anion from K₃P₇ and water in the presence of an appropriate cation sequestering agent (typically 18-crown-6 or 2,2,2-crypt).¹²⁴ We were able to extend this methodology to synthesis of the previously unreported [HAs₇]²⁻ congener in comparable yields, but all attempts to synthesize [HSb₇]²⁻ resulted only in cluster decomposition with concomitant formation of elemental antimony.¹²⁵ The bond metric data are entirely consistent with E–E single bonds, with those for [HAs₇]²⁻ elongated by

approximately 0.22 Å relative to the analogous bonds in [HP₇]²⁻. ¹H NMR data for the [HP₇]²⁻ anion show an exceptionally broad resonance centered at 0.47 ppm at room temperature attributable to the cage proton. Upon cooling to –50 °C this is resolved as a doublet of multiplets with ¹J_{H-P} = 160 Hz, collapsing to a singlet on broad-band ³¹P decoupling. The comparable resonance in [HAs₇]²⁻ occurs at 1.17 ppm.

4.2. [H₂E₇]⁻

The only report of the monoanionic [H₂P₇]⁻ cage in the literature arises from reaction of K₃P₁₁ with wet [PPh₄][Cl] in liquid ammonia.¹²⁶ It was structurally characterized as the [PPh₄]⁺ salt; however, orientational disorder within the cluster prevented the location of the hydrogen atoms and analysis of the bond metric data. This precludes identification of the isomer(s) formed (the possibility for isomerism in [E₇R_n]⁽³⁻ⁿ⁾⁻ clusters will be discussed in section 4.4). NMR data were not reported due to the compound decomposing into higher polyphosphorus species upon dissolution into dimethyl sulfoxide or acetonitrile. The presence of a P–H bond was inferred from the presence of a strong, sharp band at 2250 cm⁻¹ in the IR spectrum and the cluster charge from the X-ray crystal structure obtained. Analogous arsenic and antimony cages are currently unknown.

4.3. [H₃E₇]

The neutral heptaphosphane, [H₃P₇], is available through methanolysis of the tris(trimethylsilyl)-substituted cage, [(Me₃Si)₃P₇], in the absence of solvent.¹²⁷ When prepared in this manner, the substance is amorphous based on X-ray analysis and highly insoluble in the majority of laboratory solvents. ³¹P NMR spectroscopy studies were carried out on solutions formed directly in benzene, 1-methylnaphthalene, or 1-methylnaphthalene/phenanthrene mixtures, which have to be performed rapidly before decomposition of the compound into PH₃ and elemental phosphorus.¹²⁸ Nine apparent multiplet resonances were observed, which suggests formation of two isomers of the nortricyclane-like cage compound (vide infra). The symmetrical isomer would give rise to three resonances in a 1:3:3 intensity ratio, whereas seven equal intensity resonances would be expected for the unsymmetrical isomer. It therefore seems likely that two of the resonances overlap, giving rise to the observed nine resonances in the ³¹P NMR spectrum. A discussion on isomerism follows. As for [H₂E₇]⁻, the heavier arsenic and antimony cages are currently unknown.

4.4. Isomerism in [E₇R_n]⁽³⁻ⁿ⁾⁻ Clusters

4.4.1. [E₇R]²⁻. A general structural feature of the [E₇R]²⁻ cages (Figure 5) is their chirality due to the presence of three different substituents at the functionalized pnictide vertex (the two phosphorus atoms to which this vertex binds possess unique bonding environments). All known examples exist as racemic mixtures since no attempts have been made to separate

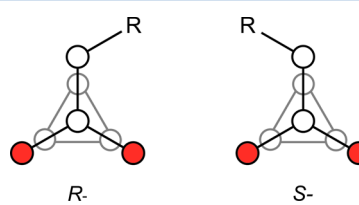


Figure 5. Two enantiomers of a monosubstituted heptaphosphide cage viewed from the apical vertex. Atoms colored in red carry a formal negative charge.

the enantiomers. Assignment of the chiral waist phosphorus atom as being of *R*- or *S*-configuration using the Cahn–Ingold–Prelog rules is nontrivial, but the basal phosphorus atom can be shown to be of higher priority than the apical phosphorus atom.

The other result of functionalization is that in the static structure there are no equivalent pnictogen atoms. All of the known $[P_7R]^{2-}$ anions display fluxionality in their ^{31}P NMR spectra, with extremely broad resonances observed at room temperature.

4.4.2. $[E_7R_2]^-$. There are three possible isomers of a disubstituted cage with two identical R groups (Figure 6). Two

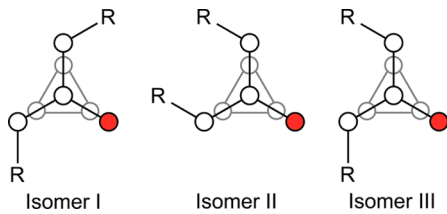


Figure 6. Representation of the three possible isomers of $[E_7R_2]^-$ viewed from the apical vertex. Atoms possessing a formal negative charge are shown in red.

(isomers I and II) possess C_s symmetry, with a mirror plane bisecting the cage between the two R groups, giving them two pairs of equivalent E atoms and three unique E atoms. The third isomer (III) has seven inequivalent E atoms. On steric grounds it seems reasonable to assume that formation of isomer I would be favored and this is generally confirmed crystallographically. It is worth noting that no evidence of fluxionality is observed in the ^{31}P NMR spectra, in contrast to the monosubstituted $[P_7R]^{2-}$ cages. Interconversion between the isomers becomes costly due to the high barriers to pyramidal inversion of the substituted atoms.

4.4.3. $[E_7R_3]$. The isomerism seen for the mono- and disubstituted cages is also possible in the trisubstituted cages, with two distinct arrangements of the R groups termed the symmetrical and unsymmetrical isomers (Figure 7). Each of

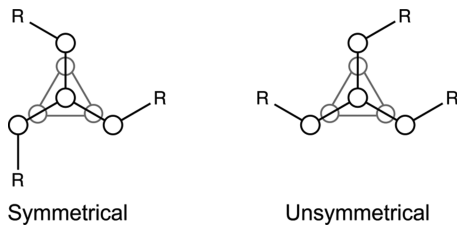


Figure 7. Two possible isomers of $[R_3E_7]$ viewed from the apical E atom. SSS (left) and RSR (right) enantiomers pictured.

these also exists as a pair of enantiomers, which can be assigned as having *R*- or *S*-configurations at the chiral phosphorus atoms using the same considerations as were used for the monosubstituted cages.

5. REACTIVITY OF $[E_7]^{3-}$ TOWARD NONMETAL MAIN-GROUP ELECTROPHILES AND $FeCp(CO)_2$

The reactivity of $[E_7]^{3-}$ seems to be best described by considering several factors. The presence of three pnictide vertices provides the cluster with a potent nucleophilicity and basicity, while the 3⁻ charge results in significant reductive

potential. In addition, the nortricylane-like geometry is relatively unstable, allowing for potential bond cleavage chemistry, which is particularly observed for the arsenic and antimony congeners on account of their weaker E–E bonds.¹¹⁴ With this in mind, the reactivity of the clusters can be broadly split into two categories: reactions where the nuclearity and (approximate) geometry of the cage is retained and reactions where the nuclearity and geometry of the cage is significantly altered.

5.1. Salt Elimination Reactions

The nucleophilic nature of the pnictide vertices allows synthesis of a series of mono-, di-, and trisubstituted cages where a two-center, two-electron exo-bond is formed between the phosphorus atom and the substituent. Examples are known for organic, main-group, and transition-metal substituents. In the latter case, the cage is described as coordinating in an η^1 mode and formally considered a two-electron donor to the metal center. Until very recently, the only synthetic method to access such cages was via salt elimination reactions between $[E_7]^{3-}$ and/or an R–X electrophile.

Monosubstituted cages, with general formula $[E_7R]^{2-}$, are rare. There are no examples for arsenic and antimony cages from salt elimination reactions, and only a handful of $[P_7R]^{2-}$ cages are known. Fritz et al. reported the observation of a $[P_7^tBu]^{2-}$ cage as a product of reaction of t^3BuLi with a cyclic tetraphosphane but did not report any characterization data.¹²⁹ The $[P_7(SiMe_3)]^{2-}$ cage can be synthesized by a ligand redistribution reaction between $[P_7(SiMe_3)_3]$ and $[P_7]^{3-}$ in a 1:2 stoichiometric ratio.¹³⁰ The only non-hydrogen-substituted crystallographically characterized $[P_7R]^{2-}$ cage, which clearly shows the racemic mixture of enantiomers formed, is with R = SiMe(SiMe₃)₂.¹³¹ This is synthesized via cleavage of two R groups from the neutral $[P_7R_3]$. At room temperature in the ^{31}P NMR spectrum “just broad signals are observed”, which resolve to seven second-order multiplets on cooling to –60 °C. Evidently a fluxional process rearranging the cage phosphorus atoms analogous to that observed for $[HP_7]^{2-}$ is operational in this cluster anion, which agrees with observations made by our research group on related systems (*vide infra*).

The most convenient synthesis of the disubstituted $[E_7R_2]^-$ cages involves transfer of an R group from a tetraalkylammonium salt, as reported by Eichhorn and co-workers (Figure 8).^{132,133} This has been used to synthesize $[E_7R_2]^-$ anions (E =

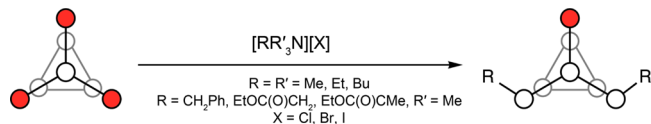


Figure 8. Synthesis of $[E_7R_2]^-$ using tetraalkylammonium salts as investigated by Eichhorn and co-workers. Atoms possessing a formal negative charge are shown in red.

P: R = Me, Et, Bu, PhCH₂, EtOC(O)CH₂, EtOC(O)CHMe; E = As: R = PhCH₂) from $[RR'_3N][X]$ salts (R = R' = Me, Et, Bu; R = PhCH₂, EtOC(O)CH₂, EtOC(O)CHMe, R' = Me; X = Cl, Br, I). The reaction is proposed to be a nucleophilic attack of a pnictide vertex of the cage at the α -carbon atom of the most electrophilic group of the ammonium salt. No evidence for a radical process was observed.

^{31}P NMR spectra of the $[P_7R_2]^-$ anions prepared by Eichhorn and co-workers displayed five resonances, which ruled out the presence of isomer III (see section 4.4.2). On

steric grounds it seems reasonable to assume that formation of isomer I would be favored, and this was confirmed crystallographically. It is worth noting that no evidence of fluxionality was observed in the ^{31}P NMR spectra, in contrast to the monosubstituted $[\text{P}_7\text{R}]^{2-}$ cages.

Reaction of $[\text{P}_7]^{3-}$ with alkyl tosylates has also been used to form $[\text{P}_7\text{R}_2]^-$ ($\text{R} = \text{'Pr}, \text{'Bu}$), and ^{31}P NMR studies suggest formation of either isomer I or isomer II.¹³⁴

Trisubstituted, neutral cages are known with organic, p-block, and transition-metal substituents, all prepared by salt metathesis with an appropriate element halide. Accordingly, the alkyl-substituted $[\text{P}_7\text{R}_3]$ ($\text{R} = \text{Me}, \text{Et}, \text{'Pr}, \text{Bu}, \text{'Bu}$),^{135–137} main-group-substituted $[\text{E}_7\text{R}_3]$ ($\text{E} = \text{P}; \text{R} = \text{SiH}_3, \text{SiH}_2\text{Me}, \text{SiMe}_3, \text{SiMe}_2\text{PEt}_2, \text{SiPh}_3, \text{GeMe}_3, \text{SnMe}_3, \text{P}'\text{Bu}_2, \text{Sb}'\text{Bu}_2; \text{E} = \text{As}; \text{R} = \text{SiMe}_3$),^{136–139} and metalated species $[\text{P}_7\{\text{Fe}(\text{Cp})(\text{CO})_2\}_3]$ are known.¹⁴⁰

Smaller R groups allow formation of both symmetrical and unsymmetrical isomers, but upon increasing the steric demands of the R group the less hindered and thermodynamically favorable symmetrical isomer is increasingly favored. For the largest R groups, such as in $[\text{P}_7\{\text{Fe}(\text{Cp})(\text{CO})_2\}_3]$, exclusive formation of the symmetrical isomer is observed. This has been argued as an example of kinetic versus thermodynamic reaction control. Since the groups are likely added sequentially, $[\text{P}_7\text{R}_2]^-$ is a probable intermediate. Only alkylation of isomer III will give the symmetrical isomer of $[\text{P}_7\text{R}_3]$, and this requires inversion of a substituted E atom in isomer I or II, a process with a high activation barrier. Accordingly, the symmetric isomer forms more slowly than the unsymmetrical isomer, despite being thermodynamically preferential, and its formation is only favored by bulky R groups.

The interatomic distances within the cage are essentially unremarkable E–E single bonds that do not vary significantly upon substitution at the pnictide vertices. The most significant change upon cluster substitution is the distance, h , between the center of the three basal atoms and the apical atom. This value increases with successive functionalization, from around 3.00 Å in $[\text{P}_7]^{3-}$ to around 3.15 Å in $[\text{P}_7\text{R}_3]$. This is in part attributable to an increase in the bond angles at the waist phosphorus atoms brought about by a reduction in electrostatic repulsion upon removal of formal negative charge on substitution.¹⁴¹

5.2. Hydropnictination Reactions

Our group has recently shown that the protic cages $[\text{HE}_7]^{2-}$ ($\text{E} = \text{P}, \text{As}$) are capable of undergoing uncatalyzed hydropnictination reactions with both carbodiimides $\text{RN}=\text{C}=\text{NR}$ ($\text{R} = \text{Dipp}, \text{Cy}, \text{'Pr}$) and isocyanates $\text{RN}=\text{C}=\text{O}$ ($\text{R} = 1\text{-adamantyl}$) (Figure 9).^{124,125,142} This results in formation of monofunctionalized cages of general formula $[\text{E}_7\text{C}(\text{NHR})(\text{NR})]^{2-}$ ($\text{E} = \text{P}, \text{As}; \text{R} = \text{Dipp}, \text{Cy}, \text{'Pr}$) from reactions with carbodiimides and $[\text{E}_7\text{C}(\text{NHR})(\text{O})]^{2-}$ ($\text{E} = \text{P}, \text{As}; \text{R} = 1\text{-adamantyl}$) from reactions with isocyanates. The mechanism for this reactivity is unknown, although deuterium-labeling studies using $[\text{DP}_7]^{2-}$ have shown that the hydrogen atom is transferred from the pnictide cage to the nitrogen atom during the course of the reaction. While it is certainly tempting to suggest that the initial step is nucleophilic attack of a cage pnictide vertex on the central carbon atom of the heteroallene, by analogy with the traditional synthesis of phosphaguanidines from carbodiimides,¹⁴³ multielement NMR studies show that the deprotonated cage $[\text{P}_7]^{3-}$ does not react with carbodiimides.

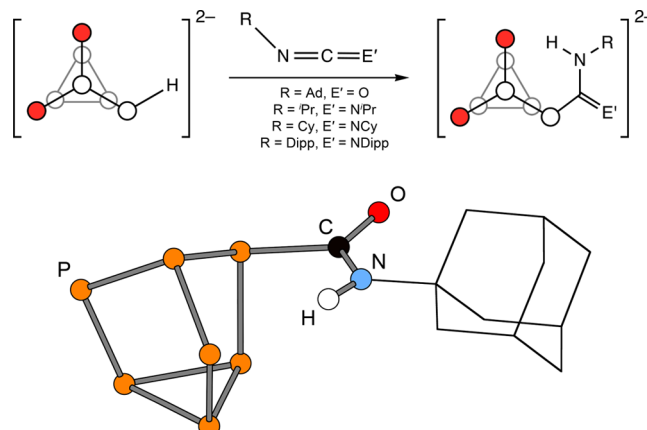


Figure 9. Hydropnictination of heteroallenes using $[\text{HE}_7]^{2-}$ cages (top). Ball and stick representation of the anion in the crystal structure of $[\text{P}_7\text{C}(\text{O})(\text{NHAd})]^{2-}$ (bottom). Atoms bearing a formal negative charge are highlighted in red.

^{31}P NMR spectra of the cages are similar to those mentioned earlier for $[\text{HP}_7]^{2-}$ and $[\text{P}_7(\text{SiMe}_3)]^{2-}$. At room temperature, the ^{31}P NMR spectra all show a multiplet resonance around 0 ppm, depending on the nature of the R group, and two extremely broad resonances centered at approximately –85 and –111 ppm. Upon cooling to –50 °C, the fluxional process is retarded and seven distinct resonances can be observed in the NMR spectrum, which arise from the seven magnetically inequivalent phosphorus nuclei. The most downfield resonances correspond to the functionalized P3 vertex (cf. Figure 2), presumably because it possesses the smallest partial negative charge (and is thus the least shielded) as a result of the functionalization.

Protonation of these amidine- and amide-functionalized cages with either mild ($[\text{NH}_4][\text{BPh}_4]$) or strong ($[\text{H}(\text{OEt})_2] \cdot [\text{BAr}^F_4]$) acids almost exclusively leads to decomposition of the P_7 cage scaffold into $[\text{P}_{16}]^{2-}$ and $[\text{P}_{21}]^{3-}$ with concomitant release of the formamidine or formamide, identified by multielement NMR spectroscopy. Presumably protonation of a phosphide vertex is followed by rapid reductive elimination of the organic fragment and oxidative coupling of the remaining phosphorus clusters. Only in the case of the very bulky $[\text{P}_7\text{C}(\text{NHDipp})(\text{NDipp})]^{2-}$ cage is it possible to isolate $[\text{HP}_7\text{C}(\text{NHDipp})(\text{NDipp})]^-$.¹²⁴ Multielement NMR spectroscopy shows formation of at least two noninterconverting isomers, likely differing only in the relative orientation of the cage proton and organic group. Computational studies suggest the four possible isomers lie close in energy, while disorder within the X-ray crystal structure precludes definitive identification of the isomers observed by NMR spectroscopy.

Reaction of $[\text{HP}_7\text{C}(\text{NHDipp})(\text{NDipp})]^-$ with a further equivalent of a carbodiimide $\text{RN}=\text{C}=\text{NR}$ ($\text{R} = \text{Dipp}, \text{Cy}, \text{'Pr}$) leads to formation of the bis(amidine)-functionalized cages $[\text{P}_7\{\text{C}(\text{NHDipp})(\text{NDipp})\}\{\text{C}(\text{NHR})(\text{NR})\}]^-$ ($\text{R} = \text{Dipp}, \text{Cy}, \text{'Pr}$). The reactions are stereoselective for the least hindered symmetrical isomer, as would be expected based on the large bulk of the Dipp groups. The ^{31}P NMR spectrum shows five apparent multiplet resonances in all cases, although for both $[\text{P}_7\{\text{C}(\text{NHDipp})(\text{NDipp})\}\{\text{C}(\text{NHR})(\text{NR})\}]^-$ ($\text{R} = \text{Cy}, \text{'Pr}$) this is due to extensive overlap between both the resonances arising from the two substituted vertices and their adjacent basal atoms, respectively.

6. COORDINATION CHEMISTRY

6.1. Review of Bonding Modes

In this report only examples where the $[E_7]^{3-}$ cages act as a two-electron donor through a pnictide vertex have been described so far. There are two other known coordination modes available to the $[E_7]^{3-}$ anion: η^2 , where it acts as a four-electron donor, and η^4 , where it acts as a six-electron donor (Figure 10). Examples are known for both coordination modes

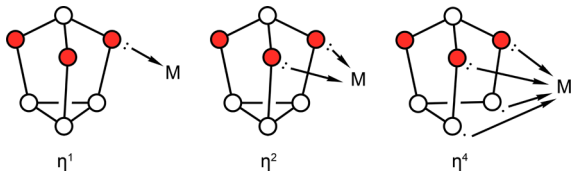


Figure 10. Diagram showing the three known bonding modes of $[E_7]^{3-}$. Atoms possessing a formal negative charge are shown in red.

from the metalation chemistry of the clusters. While the generally accepted literature term for the two-vertex binding mode has been η^2 , this implies a degree of bonding between the two coordinating pnictide vertices that is likely not present. Arguably a better description of the bonding mode could be κ^2 : the cage simply coordinates through two independent pnictide donor functionalities to a single metal center.

6.2. Structure and Bonding

6.2.1. η^2 Coordination Mode. An archetypal example of the η^2 mode is found in the $[M(\eta^2-E_7)_2]^{4-}$ ($E = P, M = Zn, Cd; E = As, M = Zn$) anions.^{144–146} These heterometallic clusters are typically synthesized by reaction of $[E_7]^{3-}$ with MPh_2 reagents in ethylenediamine. An M–C heterolytic bond cleavage is proposed, generating the phenyl anion, which has been shown to rapidly abstract a proton from the solvent to afford benzene. The structure consists of a tetrahedral M(II) d^{10} metal center coordinated by two $[E_7]^{3-}$ cages (Figure 11).

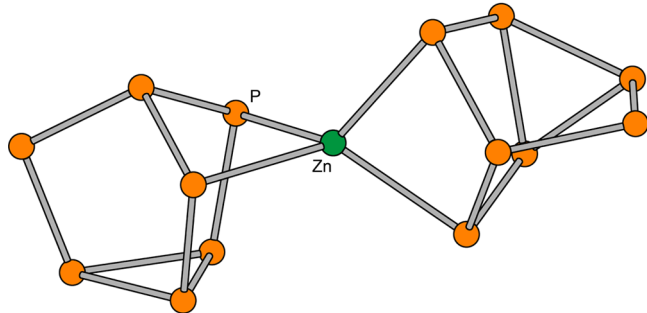


Figure 11. Synthesis and ball and stick representation of $[Zn(\eta^2-P_7)]^{4-}$.

Such an ionic description is, of course, not entirely accurate as the bonding in such clusters is highly covalent, implying a significant degree of transfer of negative charge from the cluster anions to the bridging metal (in cases in which computed Mulliken or Hirshfeld charges are reported in the primary literature; they are also discussed in this section). The cluster geometries are essentially unperturbed on coordination in this fashion, in contrast to the η^4 mode discussed below. ^{31}P NMR spectroscopy on d_5 -pyridine solutions of the $[K(2,2,2\text{-crypt})]^+$

salts of both $[Zn(P_7)_2]^{4-}$ and $[Cd(P_7)_2]^{4-}$ revealed five multiplet resonances, consistent with the pseudo C_2 point symmetry in the solid-state structure. The $[Cd(\eta^2-As_7)_2]^{4-}$ cluster anion, which possesses the same structure, can be prepared by reaction of $[As_7]^{3-}$ with $Cd(cyclohexanebutyrate)_2$ in ethylenediamine.¹⁴⁶

In contrast to these results, reaction of $HgPh_2$ with $[As_7]^{3-}$ gives rise to two distinct crystallographically characterized products, neither of which are analogous to the Cd or Zn species.^{146,147} In the presence of elemental gallium, $[Hg_2(\eta^2-E_7)_2]^{4-}$ is exclusively formed,¹⁴⁷ while reducing the stoichiometry loading of $HgPh_2:[As_7]^{3-}$ from 1:1 to 1:2 favors formation of $[HgAs(As_7)_2]^{3-}$, which is discussed in greater detail in section 6.2.2.¹⁴⁶ The $[Hg_2(\eta^2-E_7)_2]^{4-}$ anion can be considered as an $[Hg_2]^{2+}$ unit with each Hg atom coordinated in a η^2 fashion by an $[As_7]^{3-}$ cage (Figure 12).

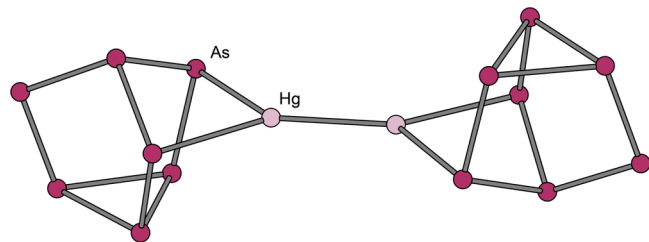


Figure 12. Synthesis and ball and stick representation of $[Hg_2(\eta^2-As_7)_2]^{4-}$.

Reaction of $[E_7]^{3-}$ ($E = P, As$) with $InPh_3$ gives rise to the $[(\eta^2-E_7)InPh_3]^{2-}$ anion (Figure 13).¹⁴⁴ In this case only one of the M–C bonds is cleaved under the reaction conditions. The related anions $[In(\eta^2-E_7)_2]^{3-}$ ($E = P, As$) can be synthesized by reaction of $[E_7]^{3-}$ solutions with $InCl_3$.¹⁴⁸ They are isostructural and isoelectronic with the aforementioned group 12 substituted anions, with an indium atom bridging two $[E_7]^{3-}$ clusters. While this can be considered in strictly ionic terms as an In^{3+} cation coordinated by two $[E_7]^{3-}$ cages, it is better regarded as a covalently bonded polyanion, with a Mulliken charge analysis on $[In(P_7)_2]^{3-}$ revealing only a modest partial positive charge (+0.3857) and significant delocalization of the cluster negative charge over the phosphorus atoms. The structure of the anion is entirely preserved in solution, with five resonances observed in the ^{31}P NMR spectrum as for the group 12 analogues. Related η^2 coordination has also been reported for the $[P_2PH_2]^{2-}$ ligand, which can be obtained via reductive coupling of white phosphorus at a niobium center.¹⁴⁹

A salt metathesis reaction between $TlCl$ and $[E_7]^{3-}$ has also been used to prepare $[Tl(\eta^2-E_7)]^{2-}$ ($E = P, As$).¹⁴⁸ Solid-state structures reveal a Tl atom coordinated in an η^2 fashion by two pnictide vertices of an $[E_7]^{3-}$ cage (Figure 13). The Tl–P_{wrist} distances in $[Tl(P_7)]^{2-}$ are 2.819(2) and 2.871(2) Å, which are significantly shorter than the distances observed between the Tl atom and the basal atoms of the phosphorus cluster (3.114(2) and 3.174(2) Å). The latter values are significantly longer than would be observed were the heptaphosphide cluster η^4 coordinated (which would result in comparable Tl–P distances). Analogous bond metric data are observed for $[Tl(As_7)]^{2-}$.

The ^{31}P NMR spectrum of $[Tl(P_7)]^{2-}$ at $-50^\circ C$ reveals two broad resonances at -99 and -147 ppm integrating in the ratio 1:2.¹⁵⁰ The missing resonance is likely obscured by a $[P_{16}]^{2-}$ impurity at ca. 60 ppm. The absence of any multiplet structure

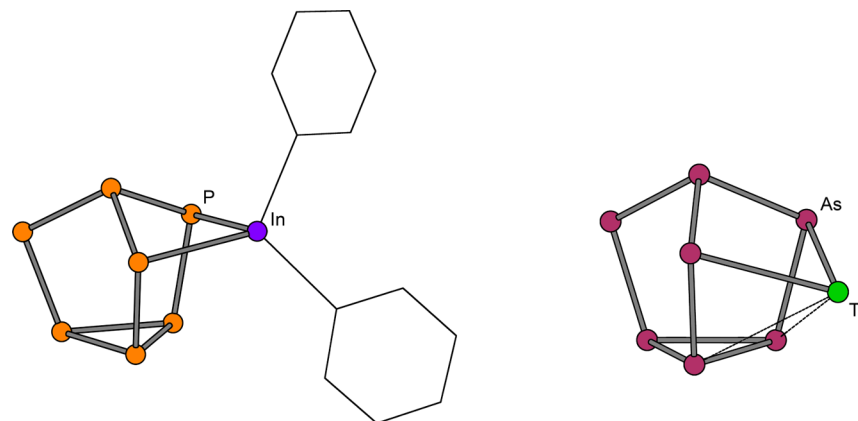


Figure 13. Ball and stick representations of $[(\text{P}_7)\text{InPh}_2]^{2-}$ (left) and $[\text{Tl}(\text{As}_7)]^{2-}$ (right).

to the two observed signals has been interpreted as indicative of an extremely facile $\eta^2\text{-}\eta^4\text{-}\eta^2$ conversion process, which is hinted at by the short Tl–P_{basal} distances in the solid-state structure.

Eichhorn and co-workers reported that reaction of ethylenediamine solutions of $[\text{E}_7]^{3-}$ ($\text{E} = \text{P}, \text{As}$) with $[\text{Pt}(\text{PPh}_3)_2(\text{C}_2\text{H}_4)]$ gives rise to the platinum complexes $[(\eta^2\text{-}\text{E}_7)\text{PtH}(\text{PPh}_3)]^{2-}$.^{151,152} Analysis by single-crystal X-ray diffraction reveals that the P and As structures are isomeric, consisting of a “PtH(PPh₃)” fragment coordinated by an intact and geometrically unaltered $[\text{E}_7]^{3-}$ cage. Through a series of competition and labeling experiments the authors have shown that the hydride ligand originates from the solvent used for reaction, with ethylenediamine proving to be the best solvent for formation of the complexes (Figure 14).

The dynamic processes occurring in $[\text{P}_7\text{PtH}(\text{PPh}_3)]^{2-}$ have been extensively studied using ³¹P NMR spectroscopic techniques and warrant comment. The limiting low-temperature spectrum displays seven multiplet resonances and a downfield broad doublet with ¹⁹⁵Pt satellites due to the PPh₃ ligand, consistent with the C₁ symmetry in the solid-state structure. Upon warming four resonances coalesce to a single broad signal, assigned to P4, P5, P6, and P7. Using a series of EXSY and ROESY experiments this has been interpreted in terms of two dynamic processes: an $\eta^2\text{-}\eta^4\text{-}\eta^2$ shifting process and a spinning step of the Pt on the P₄ face that gives rise to the apparent C₂ symmetry at room temperature.

The numbering used in Figure 14 will be used to discuss all following structures where the cage is bound in an η^4 fashion in order to keep in line with the predominant numbering scheme employed in the literature. In rare cases this does not agree with the published atom-numbering scheme—these examples will be noted and are renumbered to aid comparison between related structures.

6.2.2. Dinuclear Bridged Clusters. There are several examples known where two $[\text{E}_7]^{3-}$ cages have been found to bridge a bimetallic fragment in a $\mu,\eta^{1:1}$ coordination mode. These are structurally closely related to the previously mentioned polyphosphide $[\text{P}_{16}]^{2-}$. Replacement of one bridging P atom with an isoelectronic singly charged group 14 atom gives the $[\text{E}'\text{E}_{15}]^{3-}$ cluster anions ($\text{E} = \text{P}, \text{E}' = \text{Sn, Pb}; \text{E} = \text{As}, \text{E}' = \text{Sn}$) (Figure 15). These clusters can be synthesized by reaction of E'I₂ with $[\text{E}_7]^{3-}$ in ethylenediamine solution.¹⁴⁸ Replacement of a three-coordinate, formally neutral phosphorus atom with a formally anionic group 14 atom necessarily increases the negative charge on the cluster from 2⁻ to 3⁻. An asymmetry in the interatomic distances between the $[\text{E}_7]$

clusters and the bridging unit due to the increased size of the tetrel element would also be expected. Due to crystallographic disorder over the two bridging sites this could not be observed for $[\text{E}'\text{P}_{15}]^{3-}$, but $[\text{SnAs}_{15}]^{3-}$ was found to be fully ordered and displays the expected variation in interatomic distances. ³¹P NMR spectra of the phosphorus-containing clusters display eight resonances: seven arising from the two equivalent clusters and the eighth from the bridging phosphorus atom.

A related cluster geometry is found for $[\text{HgAs}(\text{As}_7)_2]^{3-}$, one of the products from the reaction between $[\text{As}_7]^{3-}$ and HgPh₂. This is formed exclusively when the stoichiometric loading of HgPh₂: $[\text{As}_7]^{3-}$ is altered from 1:1 to 1:2. The geometry of this anion is analogous to that of $[\text{SnP}_{15}]^{3-}$ and $[\text{P}_{16}]^{2-}$, consistent with replacement of a formally Sn(II) center with a Hg(II) atom (although the assignment of such oxidation states in a highly covalent molecule is useful only as a formalism).

Reaction of ethylenediamine solutions of $[\text{P}_7]^{3-}$ with homoleptic group 11 precursors $[\text{M}(\text{norbornene})_3][\text{SbF}_6]$ or simply MCl ($\text{M} = \text{Ag, Au}$) gives rise to the $[\text{M}_2(\text{HP}_7)_2]^{2-}$ cluster anions in low yields.¹⁵³ The yield can be significantly enhanced by addition of a proton source such as $[\text{NH}_4][\text{BPh}_4]$. By reaction of $[\text{As}_7]^{3-}$ with $[(\text{PPh}_3)\text{AuCl}]$, the deprotonated $[\text{M}_2(\text{As}_7)_2]^{4-}$ is formed instead.¹⁵⁴ Presumably the reason for formation of the protonated cages in the case of phosphorus is the significantly enhanced basicity of $[\text{P}_7]^{3-}$ as compared to $[\text{As}_7]^{3-}$, with the proton originating from the ethylenediamine solvent. The solid-state structures of all these anions reveal a $[\text{M}_2]^{2+}$ dimer bridged by two $[(\text{H})\text{E}_7]^{(2)3-}$ cages. The metals have a linear coordination environment and additionally exhibit short M–M argentophilic (2.947(1) Å) or aurophilic interactions (3.08–3.11 Å) (Figure 16).

In contrast to $[\text{P}_{16}]^{2-}$ and the related clusters discussed above, which are bent at the two central bridging phosphorus atoms, the $[\text{M}_2(\text{E}_7)_2]^{n-}$ clusters are planar at the bridged group 11 atoms (due to the absence of lone pairs at the bridged atoms). Another difference is the relative orientation of the two cages with respect to each other. In $[\text{P}_{16}]^{2-}$ the cages are both oriented in the same directions (“up-up”). In the $[\text{M}_2(\text{H})\text{E}_7]^{(2)4-}$ anionic clusters; however, the orientation is influenced by cation–anion interactions. In the case where the cations (K^+ , Rb^+ , or Cs^+) are fully sequestered by cryptand ligands and thus unable to take part in cation–anion interactions, only the opposed “up-down” isomer is observed crystallographically. However, in $\text{K}_2[\text{K}(2,2,2\text{-crypt})_2[\text{Au}_2(\text{As}_7)_2]]$ where only one-half of the cations are sequestered by cryptand ligands, As–K interactions direct the

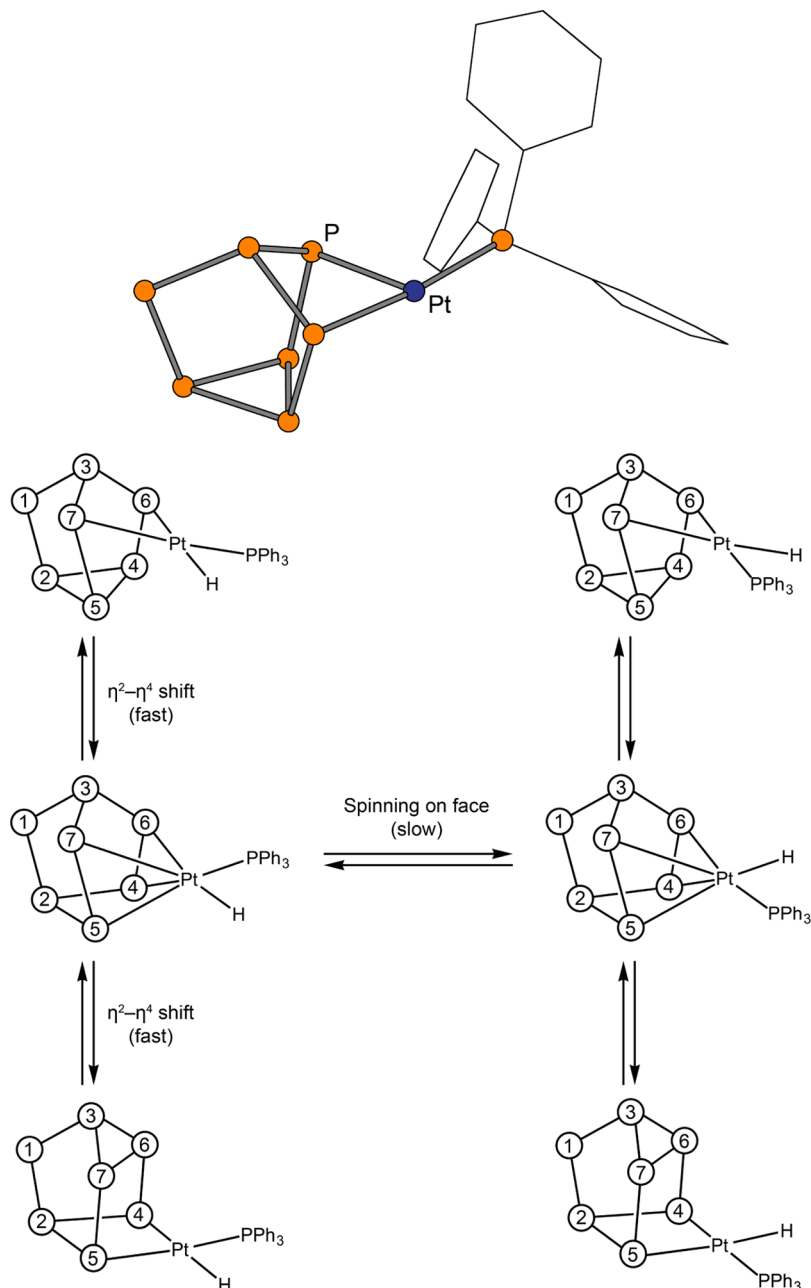


Figure 14. Structure of $[P_7PtH(PPh_3)]^{2-}$, and a summary of the dynamic processes operative in the anion as determined by ^{31}P NMR spectroscopy. Hydride ligand was not crystallographically located and has therefore been omitted in the crystal structure representation.

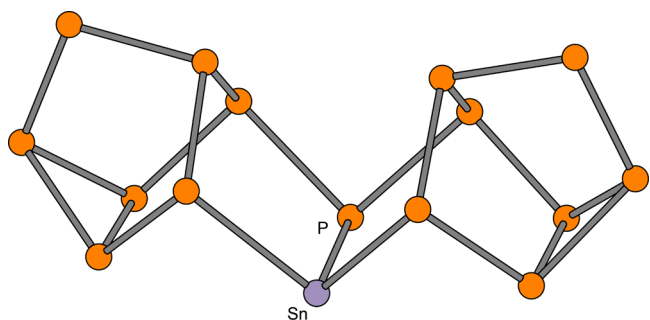


Figure 15. Ball and stick representation of $[SnP_{15}]^{3-}$.

clusters to adopt an “up–up” orientation. Calculations at the DFT level of theory on $[M_2(HP_7)]^{2-}$ place the isomers within

0.4 and 2.4 kJ mol⁻¹ for Ag and Au, respectively. Given this narrow energy gap, it is thus unsurprising that subtle cation–anion interactions can influence the solid-state orientation. Such ionic interactions are known to give rise to structural distortions in the anionic moieties of many of the binary solids discussed in section 2.

Acquisition of a ^{31}P NMR spectrum of $[M_2(HP_7)]^{2-}$ was reported to be challenging due to the combined air, moisture, and light sensitivities of the anions in solution leading to ready oxidative decomposition into $[P_{16}]^{2-}$. A spectrum could, nonetheless, be obtained that displays the expected seven multiplet resonances alongside the decomposition products.¹⁵⁰

A related copper analogue, $[Cu_2(E_7)]^{4-}$ ($E = P, As$), can be synthesized by reaction of $[P_7]^{3-}$ with $Cu_5(mes)_5$ in ethylenediamine.¹⁴⁴ The anion consists of a $[Cu_2]^{2+}$ core bridged by

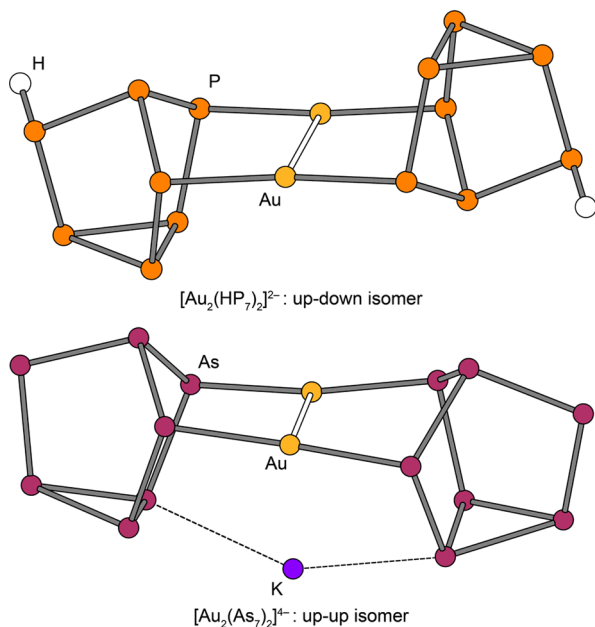


Figure 16. Ball and stick representations of the two possible cluster orientations for $[M_2(HE_7)_2]^{2-}$ (top) and $[M_2(E_7)_2]^{4-}$ (bottom) anions.

two $[E_7]^{3-}$ clusters, but instead of the symmetrical coordination observed in the case of Ag and Au, a mixed mode is observed where each Cu atom is bonded in an $\eta^{3(4)}$ fashion to one cluster and η^1 to the other cluster (Figure 17). The internuclear

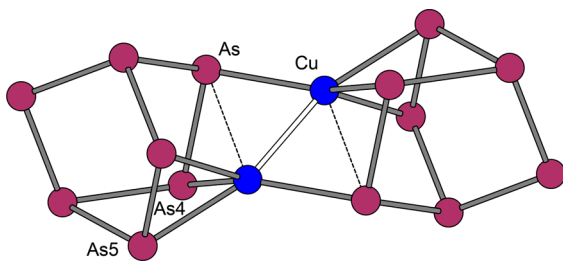


Figure 17. Ball and stick representation of $[Cu_2(P_7)_2]^{4-}$.

distances within the cluster anion are generally undistorted from that of the free cluster, with the exception of the As4–As5 bond, which is significantly lengthened to 2.772(1) Å (this atom numbering has been altered to fit that used in the section on η^4 coordination). This has been interpreted in terms of a partial nortricyclane-like to norbornadiene-like transition of the

cage, brought about by partial electron donation from the As4–As5 bond to the Cu atoms. This will be discussed in more depth below; however, the reader should note that such terms nortricyclane-like and norbornadiene-like are employed only to convey the geometry of the cluster anions and not formal negative charge (in both cases the clusters are formally 3-).

The ^{31}P NMR spectrum of $[Cu_2(P_7)_2]^{4-}$ shows evidence of two interconverting isomers. In the low-temperature limit, two separate species are observed. The first corresponds to the solid-state structure and exhibits seven well-resolved multiplet resonances. The second shows three resonances integrating in the ratio 2:1:4 and has been assigned as a fully “activated” $[Cu_2]$ dimer bridging two η^4 -coordinated norbornadiene-like $[P_7]$ clusters.

Activation of a basal bond of an $[E_7]^{3-}$ cluster in a dinuclear bridging species is observed in $[Pd_2(As_7)_2]^{4-}$, formed in the reaction between toluene solutions of $[Pd(PCy_3)_2]$ and ethylenediamine solutions of $[As_7]^{3-}$ in low crystalline yield (Figure 18).¹⁵⁵ The reaction is suggested to proceed by a “two-electron oxidation” of an intermediate species $[(\eta^2-As_7)PtH-(PCy_3)]^{2-}$ resulting in formation of H_2 . Such an intermediate is analogous to the stable cluster $[(\eta^2-P_7)PtH(PPh_3)]^{2-}$ discussed previously. The $[Pd_2(As_7)_2]^{4-}$ cluster can be considered as two square planar Pd^{2+} centers coordinated in a $\mu,\eta^{2:2}$ fashion by two $[As_7]^{4-}$ cages that display a norbornadiene-like geometry. Each Pd atom exhibits a slightly distorted square planar geometry, with an internuclear distance of 2.7144(6) Å.

6.2.3. η^4 Coordination Mode. The $[(\eta^4-E_7)M(CO)_3]^{3-}$ anions ($E = P, As$; $M = Cr, W$; $E = Sb$; $M = Cr, Mo, W$) are formed by reaction of $[E_7]^{3-}$ with metal carbonyl complexes possessing a labile ligand (mesitylene, cycloheptatriene, or 2,2'-bipyridine).^{156–158} The $[E_7]^{3-}$ cluster coordinates to the $M(CO)_3$ fragment through four of the pnictide atoms. The cage undergoes a significant structural rearrangement when coordinated in this fashion, resulting in homolytic cleavage of an E–E bond in the basal triangle to give a norbornadiene-like geometry. The true degree of bond activation to a perfectly norbornadiene-like geometry depends on the identity of both the metal and the pnictogen cage being considered. Full cluster oxidation would break the E–E bond in the base of the cluster (here numbered E4–E5), donating all of the electron density to the $M(CO)_3$ fragment, and necessarily distorting the cage geometry. This can be reflected in the relative E4–E5 and E6–E7 distances, which should be identical in the case of total activation. In all of the $[(E_7)M(CO)_3]^{3-}$ cages so far synthesized, there is a slight asymmetry in the E4–E5 and E6–E7 distances (Δd_{E-E} 0.20–0.35 Å). The smallest asymmetry is found for $[(\eta^4-As_7)Cr(CO)_3]^{3-}$, which has been

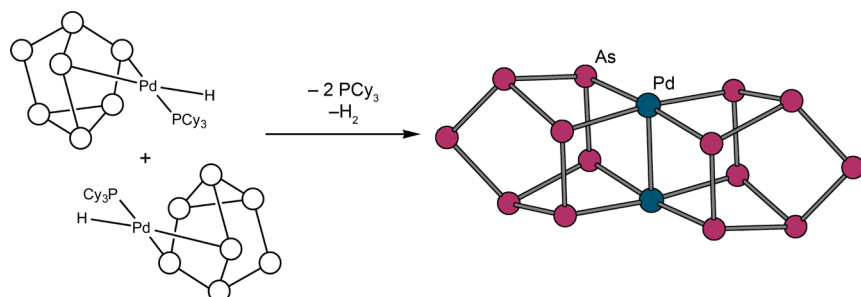


Figure 18. Proposed intermediate and structure of $[Pd_2(As_7)_2]^{4-}$. Proton source for H_2 formation in this reaction was found to be the reaction solvent (ethylenediamine).

attributed to the metal and cage being of optimal size for the best orbital overlap. The CO stretching frequencies are low, indicating substantial charge transfer from the negatively charged cage to the $M(CO)_3$ fragment.

Cleavage of a basal bond results in the cage being considered a six-electron donor to the metal center, through two pnictide vertices and two pnictinyl donors. However, this formalism is not a good descriptor of the bonding between such cages and metal centers. Fenske–Hall molecular orbital calculations on the $[(\eta^4-E_7)Cr(CO)_3]^{3-}$ complexes using both the idealized C_{2v} geometry and the C_s symmetry observed for the experimental structures show significant similarities between $[(\eta^4-E_7)]^{3-}$ and the cyclobutadiene fragment (Figure 19).¹⁵⁷ The major

Fenske–Hall may now be somewhat outdated, more recent studies using density functional theory (DFT) generally agree with this bonding picture.

This distorted structure is not preserved in solution. ^{31}P NMR studies on $[(\eta^4-P_7)Cr(CO)_3]^{3-}$ show three resonances integrating in a 1:2:4 ratio, which indicates that all four metal-bound phosphorus atoms are equivalent on the NMR time scale. Even on lowering the temperature the virtual C_{2v} structure is retained, indicating a rapid fluxional “wagging” process exchanging the phosphorus atoms.

The presence of a pnictide vertex on the $[E_7]^{3-}$ cluster allows further nucleophilic chemistry of these anions to be explored (Figure 20). The $[(\eta^4-P_7)M(CO)_3]^{3-}$ ($M = Cr, W$) clusters can be readily protonated in ethylenediamine with weak acids such as 9-phenylfluorene to form $[(\eta^4-HP_7)M(CO)_3]^{2-}$ ($M = Cr, W$).¹⁵⁹ These protonated anions can also be synthesized by treating $[(\eta^4-P_7)M(CO)_3]^{3-}$ with I_2 via an oxidation/hydrogen atom abstraction process. Treatment of the protonated anions with MeO^- results in quantitative deprotonation to reform $[(\eta^4-P_7)M(CO)_3]^{3-}$. The 1H NMR spectrum of $[(\eta^4-HP_7)Cr(CO)_3]^{2-}$ displays a doublet of multiplets centered at 4.8 ppm, and in the ^{31}P NMR spectrum four resonances are observed in a 2:2:2:1 ratio. This is consistent with the breaking of pseudo C_{2v} symmetry upon protonation at P1, making the P4/P6 and P5/P7 pairs of atoms inequivalent.

The phosphide vertex can also be substituted by metals to form bimetallic anions $[(en)(CO)_3W(\eta^1,\eta^4-P_7)M(CO)_3]^{3-}$ ($M = Cr, W$),^{157,160} or main-group electrophiles to make $[(\eta^4-RP_7)W(CO)_3]^{2-}$ ($R = PhCH_2, Me_3Si, ^nBu_3Si, Hex_3Si, Ph_3Si, Et_3Ge, Ph_3Ge, Et_3Sn, ^nBu_3Sn, Cy_3Sn, Ph_3Sn, Ph_3Pb$).¹⁶¹ Variable-temperature ^{31}P NMR studies on these compounds reveal that, in contrast to $[(\eta^4-HP_7)W(CO)_3]^{2-}$, the barrier to pyramidal inversion at P1 is remarkably low, and at room temperature all metal-bound phosphorus atoms are rendered equivalent.

In contrast to the cage-based reactivity with electrophiles, metal-based reactivity of $[(\eta^4-P_7)M(CO)_3]^{3-}$ ($M = Mo, W$) is observed with carbon monoxide. Under 1 atmosphere of gas, CO is bound at the metal center accompanied by a change of cage hapticity to form $[(\eta^2-P_7)M(CO)_4]^{3-}$ anions.¹⁶² A direct synthetic route is feasible by reaction of $[P_7]^{3-}$ with $W(CO)_4$ (pyridine)₂, but the reaction is reported to proceed very slowly at room temperature, and heating results in decarbonylation of the product to form the η^4 -bound cage. Five multiplet resonances are observed in the ^{31}P NMR spectra of the η^2 complexes, as would be expected based on the C_s symmetry of the complexes in the solid state. The η^2 complexes react with proton sources and ammonium salts similarly to the η^4 complexes to give cages that are protonated or alkylated, respectively, at P1. Upon this substitution, the mirror plane of symmetry bisecting the cage is lost and so the ^{31}P NMR spectra of such complexes display seven multiplet resonances corresponding to the seven inequivalent phosphorus atoms.

A related Ni(CO) complex is formed in the reaction of $[P_7]^{3-}$ with $[Ni(CO)_2(PPh_3)_2]$ in ethylenediamine to form $[(\eta^4-P_7)Ni(CO)]^{3-}$.¹⁵¹ The anion has pseudo C_{2v} symmetry in the solid state, with P4–P5 and P6–P7 distances of 2.952(5) and 3.005(5) Å, respectively. The similarity of these distances shows that the cage has effectively been fully activated from a nortricyclane-like to norbornadiene-like geometry, in contrast to the group 6 metal complexes discussed above. The ^{31}P NMR spectrum shows three resonances integrating in a 1:2:4 ratio, consistent with the solid-state structure. Treatment of ethyl-

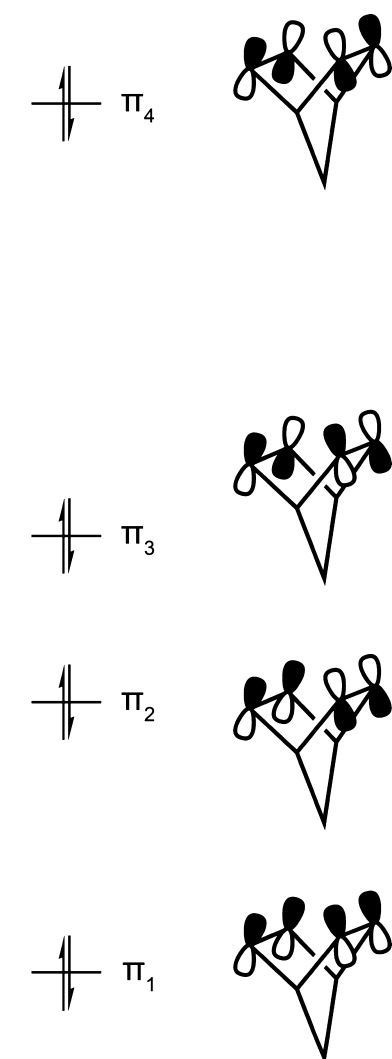


Figure 19. Simplified molecular-orbital diagram for $[(\eta^4-E_7)]^{3-}$. In the case of Sb the relative energies of π_2 and π_3 are reversed, which has been attributed to poorer π overlap on descending the group (a consequence of the so-called double-bond rule).

interactions between the cage and the metal are of π -type symmetry, with the primary interactions between the π_2 and π_3 orbitals of the cage with the $M(CO)_3$ fragment. Upon moving from undistorted C_{2v} to C_s symmetry the total energy of the cluster is lowered due to additional orbital mixing within the cluster. This distortion has been attributed to a second-order Jahn–Teller effect. While semiempirical methods such as

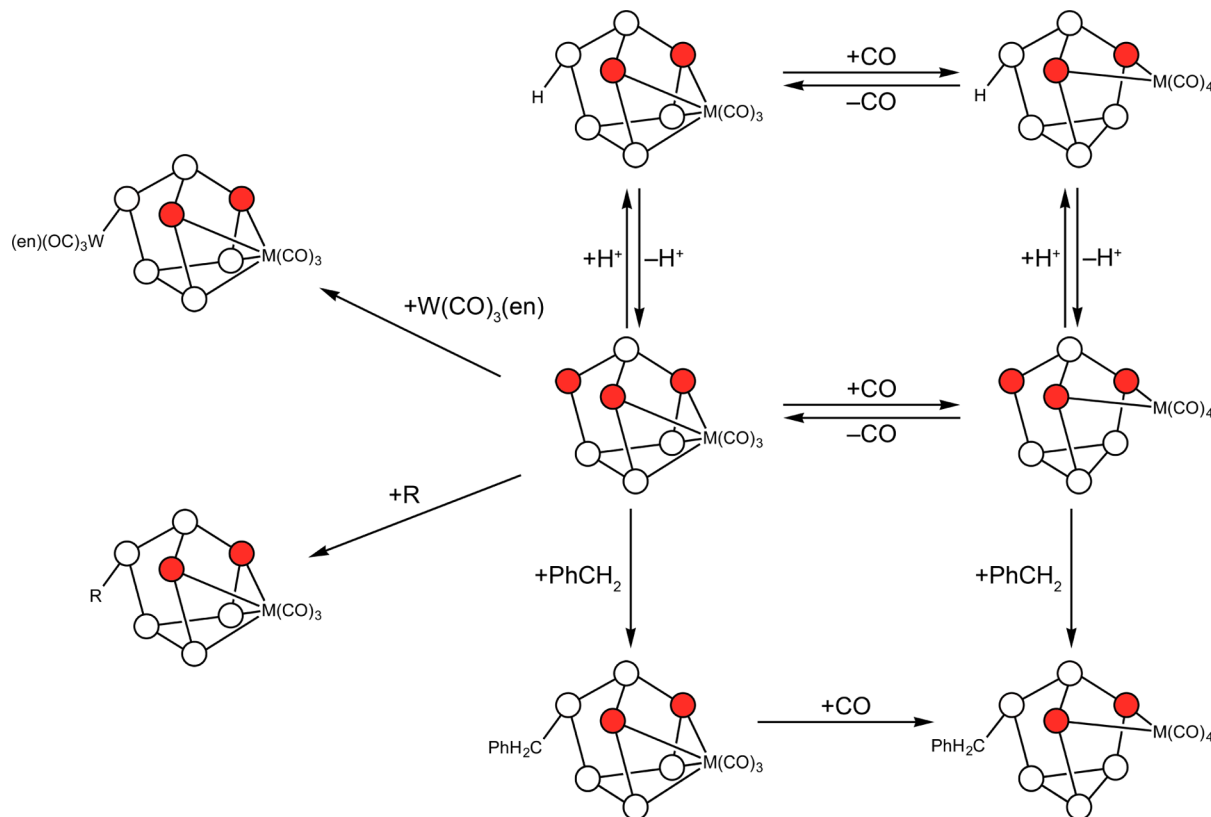


Figure 20. Summary of the chemistry with electrophiles available to $[(E_7)M(CO)_3]^{3-}$ clusters. Atoms shown in red possess a formal negative charge. $[(E_7)M(CO)_3]^{3-}$ clusters can be protonated using 9-phenylfluorene but not methanol, whereas $[(E_7)M(CO)_4]^{2-}$ are more basic and can be protonated using methanol.

enediamine solutions of $[(\eta^4\text{-P}_7)\text{Ni}(\text{CO})]^{3-}$ with methanol forms the protonated species $[(\eta^4\text{-HP}_7)\text{Ni}(\text{CO})]^{2-}$ quantitatively. The identity of this anion has been established by ^1H and ^{31}P NMR spectroscopy, which unequivocally locates the proton on P1, in contrast to the electronically equivalent anion $[(\eta^4\text{-P}_7)\text{PtH}(\text{PPh}_3)]^{2-}$ which is protonated at the metal center.

Homoleptic $\eta^4\text{-}[E_7]$ complexes are rare, with only one example known. The ferrocene analogue $[\text{Fe}(\eta^4\text{-HP}_7)_2]^{2-}$ is made in low yields from reaction between FeCl_2 and $[\text{P}_7]^{3-}$ in ethylenediamine.¹⁶³ The proton was assumed to originate from adventitious moisture in the solvent, and addition of a weak proton source ($[\text{NH}_4]^+$) allowed the yield to be significantly enhanced. The cluster anion consists of a central Fe atom coordinated by two $[\text{HP}_7]^{2-}$ cages in an η^4 fashion (Figure 21). Crystallographic disorder prevents the resolution of the cages as either being in the staggered or eclipsed conformations, although DFT level calculations suggest that the staggered optimized geometry is approximately 40 kJ mol⁻¹ lower in

energy than the eclipsed isomer. The $^{31}\text{P}\{\text{H}\}$ NMR spectrum shows four resonances integrating in the ratio 1:2:2:2. The simplicity of the observed spectrum indicates that there is fast rotation of the $[\text{HP}_7]^{2-}$ cluster cages, making both cages magnetically equivalent (analogously to what is observed for cyclopentadienyl or tris-pyrazolylborate complexes). Analysis of the ^1H NMR spectrum reveals a resonance at 6.54 ppm with $J_{\text{P}-\text{H}} = 169$ Hz, confirming direct attachment of the proton to the cage.

Oxidative coupling of two $[\text{P}_7]^{3-}$ cages to a $[\text{P}_{14}]$ cage has been observed in the reaction of $[\text{NiCl}_2(\text{P}^n\text{Bu}_3)_2]$ with $[\text{P}_7]^{3-}$ in ethylenediamine solution.¹⁴⁰ This reaction gives rise to the $[\{\text{Ni}(\text{P}^n\text{Bu}_3)_2\}_2\text{P}_{14}]$ cluster, in which two activated, norbornadiene-like clusters are linked through the unique phosphorus atom (Figure 22). Two unique nickel environments can be identified: one coordinated in an η^4 fashion through P4/P6 and P5/P7 and the second η^2 by P4/P6 and η^1 in a traditional phosphine-like coordination by P1 (atom numbering has been altered to be consistent with that used in the rest of this section). Five resonances are observed in the ^{31}P NMR spectrum, four of which are assigned to the P_{14} cage, suggesting that the solid-state structure is retained upon solvation.

7. CLUSTER FRAGMENTATION AND REARRANGEMENT

7.1. Metal-Mediated Activation

While η^4 coordination of the cluster can be considered a mild activation of the cage, there are also examples known where the geometry or indeed the nuclearity of the cage is significantly altered. Until recently all known examples were for the heavier

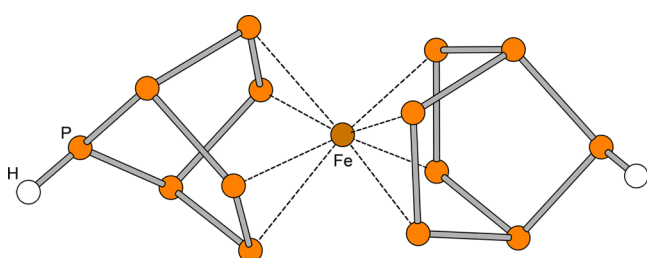


Figure 21. Ball and stick representation of $[\text{Fe}(\eta^4\text{-HP}_7)_2]^{2-}$.

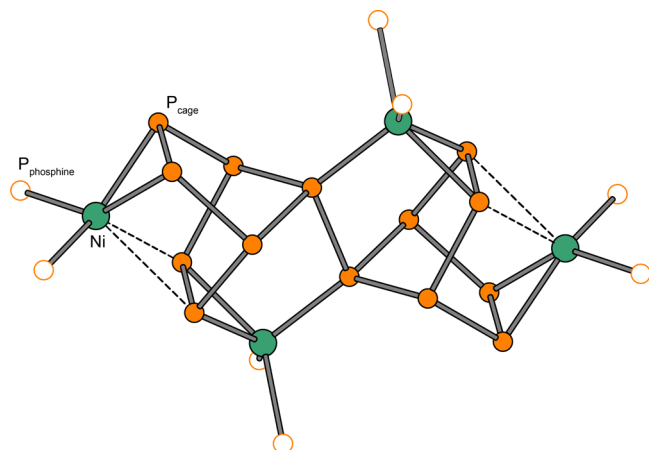


Figure 22. Ball and stick representation of $\{[\text{Ni}(\text{P}^{\text{n}}\text{Bu}_3)_2\}_{4}\text{P}_{14}\}$. ^nBu groups have been removed for clarity.

arsenic and antimony congeners. Indeed, the only known examples of an intact $[\text{Sb}_7]^{3-}$ cage (beyond simple alkali metal salts) are the $[(\eta^4\text{-Sb}_7)\text{M}(\text{CO})_3]^{3-}$ anions. This behavior is likely attributable to the necessary requirement for bond cleavage on cluster dissociation and reassembly. On descending group 15 the E–E bond dissociation energies are known to decrease, allowing for more facile cluster rearrangements. This is taken to its logical conclusion in the chemistry of the homoatomic bismuth polyanions $[\text{Bi}_4]^{2-}$ and $[\text{Bi}_2]^{2-}$ (no $[\text{Bi}_7]^{3-}$ cluster is known in either the solid-state or solution)^{56,62,63} or their bimetallic extensions as $[\text{Bi}_2\text{E}'_2]^{2-}$ or $[\text{Bi}_3\text{E}''_2]^{2-}$ ($\text{E}' = \text{Sn}, \text{Pb}; \text{E}'' = \text{Ga}, \text{In}$)^{164–166,217} all of which give rise to large heterometallic systems on reaction with transition-metal reagents.^{166–177}

The reaction mechanisms that give rise to higher nuclearity clusters are poorly understood, yet occasionally well-defined products can be isolated. A series of $[\text{ME}_8]^{n-}$ ($\text{M} = \text{Nb}, \text{Cr}, \text{Mo}; \text{M} = \text{As}, \text{Sb}; n = 2, 3$) are synthesized either by reaction of $[\text{E}_7]^{3-}$ with $[\text{M}(\text{arene})_2]$ complexes in the presence of 2,2-crypt or in a solid-state synthesis.^{178–181} These comprise a crown-like E_8 ring possessing a formal 8– charge, isolobal and isoelectronic with S_8 , centered by a metal cation that is formally in the +5 or +6 oxidation state for electron counting purposes (Figure 23). To date, $[\text{NbE}_8]^{3-}$ ($\text{E} = \text{As}, \text{Sb}$), $[\text{MoAs}_8]^{2-}$,

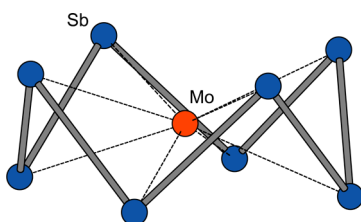


Figure 23. Ball and stick representation of the $[\text{MoSb}_8]^{3-}$ anion.

$[\text{MoSb}_8]^{3-}$, and $[\text{CrAs}_8]^{2-}$ have been synthesized and crystallographically characterized. Structural analysis of these anions reveals the surprising degree of flexibility inherent to the E_8 ring. In order to accommodate metals of varying sizes, the ring can pucker, reducing the E–E–E angles from $93.7(1)^\circ$ in $[\text{NbAs}_8]^{3-}$ to $89.5(2)^\circ$ in $[\text{CrAs}_8]^{2-}$. This is also accompanied by a slight reduction in E–E bond lengths. Taken together these two factors likely explain the inability to synthesize $[\text{CrSb}_8]^{n-}$; it is simply not possible to contract the Sb–Sb

bonds and angles sufficiently to overlap with the much smaller interstitial Cr atom. Computational studies at the DFT level of theory on the series $[\text{MAS}_8]^{n-}$ ($\text{M} = \text{V}, \text{Nb}, \text{Ta}, \text{Cr}, \text{Mo}, \text{W}, \text{Mn}, \text{Tc}, \text{Re}$) reveal that this ring puckering is concomitant with an increase in covalency across the period.¹⁸²

Calculations have shown that there is significant π donation from the pnictide ring to the metal center, as would be expected for a metal center in such a high formal oxidation state. The LUMO in all systems is predominantly composed of metal d_{z^2} character. The HOMO consists of the lone pairs on the E atoms, which form an orbital with high electron density on both faces of the crown, each composed of four E lone pairs. This orbital allows selective binding of large (Rb^+, Cs^+) alkali metal cations in the presence of excess Na^+ and K^+ , as studied by ESI-MS,¹³³ Cs^{133} NMR spectroscopy, and crystallization experiments.

The $[\text{As}@\text{Ni}_{12}@\text{As}_{20}]^{3-}$ cluster is synthesized by reaction of $[\text{Ni}(\text{COD})_2]$ with $[\text{As}_5]^{3-}$.¹⁸³ The geometry of this remarkable cluster consists of an icosahedral $[\text{Ni}_{12}(\mu^{12}\text{-As})]^{3-}$ core encapsulated in a near undistorted fullerene-like pentagonal dodecahedral As_{20} unit, with the cluster possessing overall I_h symmetry (Figure 24). The As_{20} unit is electron precise,

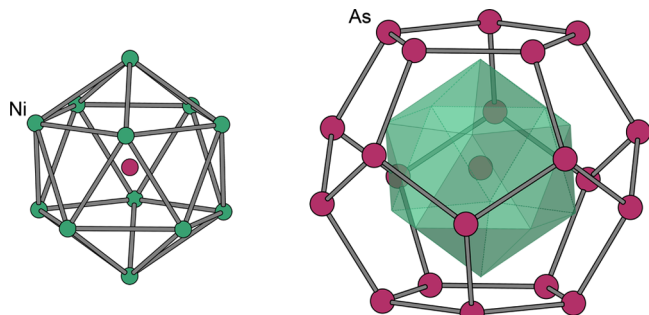


Figure 24. Ball and stick representation of the $[\text{As}@\text{Ni}_{12}]$ core (left) and its relation to the overall cluster geometry (right).

possessing 100 valence electrons that are split between 30 As–As bonds and 20 lone pairs present in the p_z orbitals. Extended Hückel calculations reveal that the interaction between this framework and the $[\text{Ni}_{12}(\mu^{12}\text{-As})]^{3-}$ center is between the arsenic lone pairs and the Ni_{12} virtual orbitals that are mainly p orbital in character. The As–As bonding finds negligible overlap and is essentially unaffected.

An analogous reaction between $[\text{Ni}(\text{COD})_2]$ and $[\text{Sb}_7]^{3-}$ gives rise to $[\text{Ni}_5\text{Sb}_{17}]^{4-}$, which possesses an entirely different structure (Figure 25).¹⁸⁴ The heterometallic cluster can be considered to consist of an Sb_{13} bowl that is coordinated to a $[\text{Ni}(\text{cyclo-Ni}_4\text{Sb}_4)]$ unit. The Sb–Sb bonding falls into two classes: primary bonds with distances lying in the range $2.816(4)$ – $2.928(4)$ Å and secondary contacts in the range $3.095(2)$ – $3.176(2)$ Å indicative of weak interactions. A cluster electron count gives 139 valence electrons, with DFT calculations pointing to an $S = 3/2$ ground state. Despite very similar reaction conditions to the aforementioned $[\text{As}@\text{Ni}_{12}@\text{As}_{20}]^{3-}$ being used entirely disparate products are obtained, hinting at the possibility that multiple reaction products can arise from such reactions and that only those that crystallize readily are isolated.

A cluster, $[\text{Pd}_7\text{As}_{16}]^{4-}$, that possesses structurally similar elements is reproducibly found as a side product in the synthesis of $[\text{Pd}_2(\text{As}_7)]^{4-}$.¹⁵⁵ In this case the structure can be considered as a $[\text{Pd}_2\text{As}_{12}]$ bowl capped by a $[\text{Pd}(\text{cyclo-Pd}_4\text{As}_4)]$

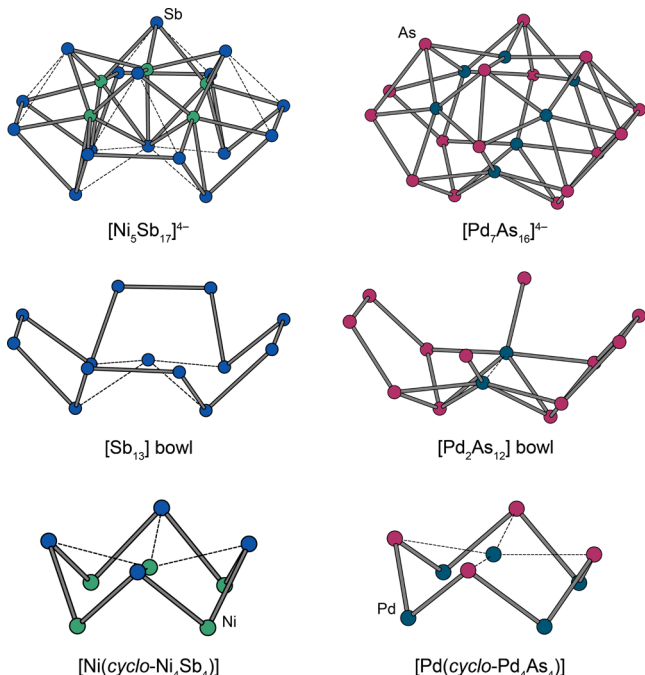


Figure 25. Ball and stick representations of $[Ni_5Sb_{17}]^{4-}$ and $[Pd_7As_{16}]^{4-}$, highlighting the structural similarities.

unit that is topologically identical to the $[Ni(cyclo-Ni_4Sb_4)]$ unit in $[Ni_5Sb_{17}]^{4-}$. In $[Ni(cyclo-Ni_4Sb_4)]$, the central metal atom sits in the center of the crown-like Ni_4Sb_4 ring ($Ni-Sb = 2.59(3)$ Å (av), $Ni-Ni = 2.56(3)$ Å (av)), whereas in $[Pd(cyclo-Pd_4As_4)]$ the central Pd atom makes significantly shorter bonds to the As atoms ($Pd-As = 2.57(5)$ Å (av) relative to the ring Pd atoms ($Pd-Pd = 2.85(3)$ Å). The seven palladium atoms exhibit a geometry that is approximately a distorted capped trigonal antiprism, which for electron counting purposes can be considered to consist of six Pd(I) centers and one Pd(II) center. The interatomic distances within this subunit lie in the range $2.800(1)$ – $2.907(1)$ Å, which is consistent with those found in other Pd clusters.¹⁸⁵

A further example can be found in the reaction of $[Ni(CO)_2(PPh_3)_2]$ with $[Sb_7]^{3-}$. Earlier, we discussed how the reaction of this transition-metal compound with $[P_7]^{3-}$ gave rise to the $[(\eta^4-P_7)Ni(CO)_3]^{3-}$ cluster.¹⁵¹ In contrast, reaction with $[Sb_7]^{3-}$ results in formation of the 10-vertex $[Sb_7Ni_3(CO)_3]^{3-}$ cluster with pseudo- C_s point symmetry (Figure 26).¹⁸⁶ Electron counting gives 24 cluster electrons, consistent with a $(2n + 4)$ *nido* cluster using the Wade–Mingos rules.^{187–190} Alternatively, it can be viewed as an electron-precise $[Sb_7Ni(CO)]^{3-}$ core (with 12 two-center two-electron bonds) with two open faces capped by $Ni(CO)$ units. The reaction is postulated to proceed via an $[(\eta^4-Sb_7)Ni(CO)]^{3-}$ intermediate, analogous to the $[(\eta^4-P_7)Ni(CO)]^{3-}$ cluster discussed earlier (vide supra), that further inserts $Ni(CO)$ units to give the final product.

Reaction between $[As_7]^{3-}$ and $[CoCl_2(PEt_2Ph)_2]$ gives rise to the neutral, ligand-supported $[Co_6As_{12}(PEt_2Ph)_6]$ cluster.¹⁴⁰ The product consists of a Co_6As_6 heteroicosahedron formed of a chairlike As_6 ring with Co_3 triangles completing the icosahedron, with As_3 units capping the Co_3 faces to give octahedra. Each cobalt atom has its coordination sphere completed by a supporting PEt_2Ph ligand. Overall, the cluster has approximate D_{3d} symmetry. Computational analysis shows

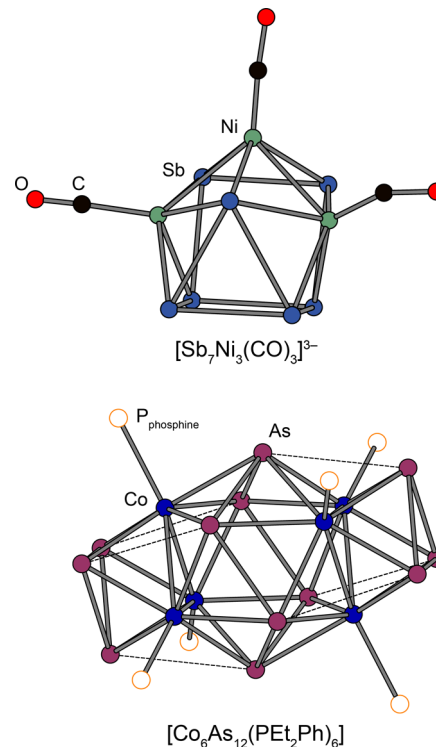


Figure 26. Ball and stick representations of the ligand-supported clusters $[Sb_7Ni_3(CO)_3]^{3-}$ and $[Co_6As_{12}(PEt_2Ph)_6]$. All organic phosphine substituents from $[Co_6As_{12}(PEt_2Ph)_6]$ are omitted for clarity.

that the cage is diamagnetic, with the high degree of covalency resulting in delocalized valence molecular orbitals. The cage has 38 skeletal electrons, consistent with a $(2n + 2)$ electron count for an 18-atom polyhedral cage.

It is also worth noting that transformations involving the metal-mediated cluster activation of neutral exo-functionalized clusters such as $[P_7(SiMe_3)_3]$ or $[As_7(SiMe_3)_3]$ has also been demonstrated by Fenske and co-workers.^{140,191,192}

As mentioned above, cluster fragmentation reactions are virtually unknown for $[P_7]^{3-}$. The cobalt organometallic compound $[Co(mes)_2(PPhEt_2)_2]$ has recently been reported to activate both the $[P_7]^{3-}$ and the $[As_7]^{3-}$ cages.^{193,194} The products resulting from this transformation are $[Co(\eta^5-P_5)\{\eta^2-P_2H(mes)\}]^{2-}$ and $[Co(\eta^3-As_3)\{\eta^4-As_4(mes)_2\}]^{2-}$, respectively (Figure 27). In both cases, the nuclearity (i.e., seven) of the parent cluster has been maintained, but extensive cage rearrangement has occurred. The former transformation is also the first example of the chemical activation of the naked $[P_7]^{3-}$ cage. These molecules contain pnictide analogues of organic ligands, namely, $[P_5]^-$ (cyclopentadienide, Cp , $[C_5H_5]^-$), $[HP=P(mes)]$ (alkenes, $R_2C=CR_2$), and $[As_4R_2]^{2-}$ (butadiene, C_4R_6). The ^{31}P NMR spectrum of $[Co(\eta^5-P_5)\{\eta^2-P_2H(mes)\}]^{2-}$ shows three signals at 158, -13, and -106 ppm integrating in the ratio 5:1:1, which are assigned to the $[P_5]^-$ unit, the $P(mes)$ of the diphosphene, and the PH of the diphosphene, respectively.

7.2. Activation by Unsaturated Organic Substrates

Our group has recently become interested in the reactivity of $[E_7]^{3-}$ toward unsaturated organic molecules, in particular as a source of anionic $[E_n]$ fragments for synthesis of phosphorus-containing analogues of common organic molecules. This area

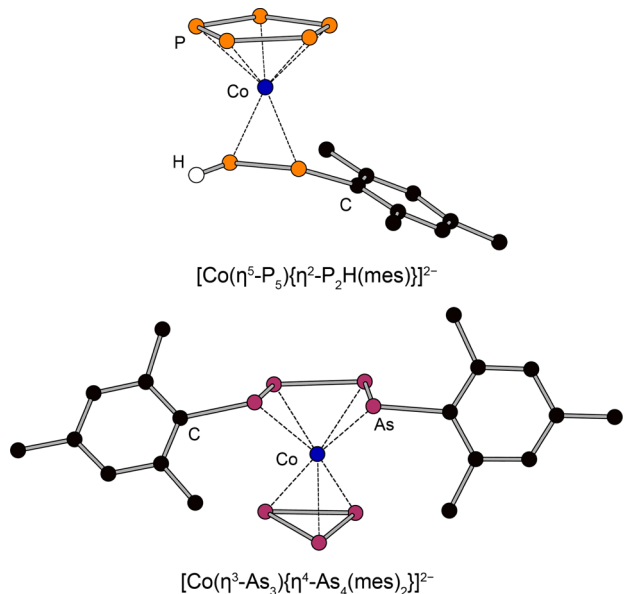


Figure 27. Ball and stick representations of $[\text{Co}(\eta^5\text{-P}_5)\{\eta^2\text{-P}_2\text{H}(\text{mes})\}]^{2-}$ and $[\text{Co}(\eta^3\text{-As}_3)\{\eta^4\text{-As}_4(\text{mes})_2\}]^{2-}$.

of chemistry has been extensively documented and termed “phospha-organic” chemistry.^{195,196}

$[\text{E}_7]^{3-}$ ($\text{E} = \text{P}, \text{As}$) clusters react with alkynes with transfer of an $[\text{E}_3]^{-}$ unit to form an unusual class of cyclopentadienide analogue, the 1,2,3-tripnictolides $[\text{1,2,3-E}_3\text{C}_2\text{RR}']^-$ ($\text{E} = \text{P}, \text{As}$, $\text{R} = \text{H}, \text{R}' = \text{H}, \text{Ph}$, 2-pyridyl; $\text{R} = \text{Ph}, \text{R}' = \text{Ph}$) (Figure 28).^{197–200} Synthetic methods for synthesis of this class of

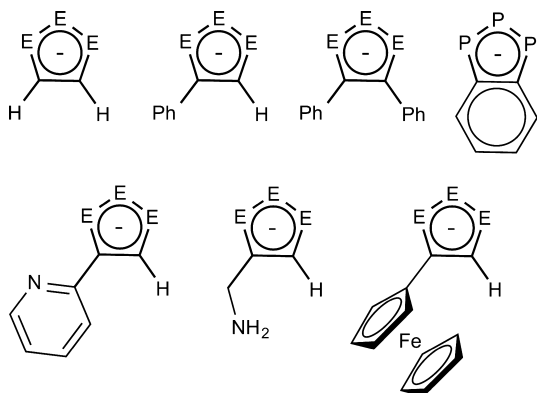


Figure 28. Range of 1,2,3-tripnictolide anions accessible through the “Zintl anion” methodology ($\text{E} = \text{P}, \text{As}$).

compound remain underdeveloped, with only a few examples existing in the literature.^{65,96,201–205} The reaction mechanism that gives rise to such species from $[\text{E}_7]^{3-}$ is unknown, although the outcome is reminiscent of a 1,3-dipolar cycloaddition (“click”) reaction between an alkyne and an azide to give a triazole.²⁰⁶ Depending on the alkyne used, the reaction is not specific for formation of the 1,2,3-tripnictolide, and multiple other unidentified phosphorus-containing side products can be observed in the crude ${}^{31}\text{P}$ NMR spectra. Presumably the driving force for formation of the 1,2,3-tripnictolide anions is their aromaticity.

The triphospholides are characterized by downfield-shifted resonances in their ${}^{31}\text{P}$ NMR spectra between 260 and 340 ppm with a distinct A_2B splitting pattern. The proton

resonances are similarly downfield shifted, with the triphospholides and triarsolides appearing around 9.5 and 10.5 ppm, respectively. X-ray structural analyses reveal planar monoanions with interatomic distances intermediate between those for $\text{E}-\text{E}$, $\text{E}-\text{C}$, and $\text{C}-\text{C}$ double and single bonds, as would be expected on the basis of their aromaticity.

Other work on unsaturated substrates has investigated the reactivity of $[\text{P}_7]^{3-}$ toward carbon monoxide. No reactivity is observed at room temperature, but in refluxing DMF good yields of the phosphaethynolate anion, $[\text{PCO}]^-$, can be formed as the $[\text{K}(18\text{-crown-6})]^+$ salt.²⁰⁷ This anion has previously been reported by Becker and co-workers²⁰⁸ and the synthesis recently refined by the group of Grützmacher involving reaction of NaPH_2 with diethylcarbonate.^{209,210} These facile syntheses have inspired renewed interest in this small molecule, from computational analyses of its bonding and reactivity,^{211,212} to its use in heterocycle synthesis,^{207,208,210,213,214} to fundamental comparisons with lighter congeners.^{215,216}

8. CONCLUSION

Recent breakthroughs in the solution-phase reactivity of heptapnictide trianions have shown that such species may be used for generation of novel organopnictogen compounds. By analogy with the chemistry of white phosphorus, it is clear that the controlled chemical transformation of $[\text{E}_7]^{3-}$ may be employed as a viable synthetic protocol for synthesis of families of otherwise elusive compounds such as $[\text{E}_3\text{C}_2\text{RR}']^-$ or PCO^- . These recent discoveries bode well for a research area that straddles both solution-phase and solid-state chemistry and demonstrate that $[\text{E}_7]^{3-}$ clusters may be more than simple chemical curiosities but rather unique chemical feedstocks.

AUTHOR INFORMATION

Corresponding Author

*E-mail: jose.goicoechea@chem.ox.ac.uk.

Author Contributions

The manuscript was written through contributions of all authors. All authors have given approval to the final version of the manuscript.

Notes

The authors declare no competing financial interest.

Biographies



Robert Turberville obtained his undergraduate degree from the University of Oxford. He started his research career with a summer project in the group of Professor Stephen Faulkner working on luminescent lanthanide complexes, before moving on to work on

main-group N-heterocyclic carbene complexes with Jose Goicoechea for his final year (Part II) project. Remaining in the Goicoechea group for his graduate studies, he received his D.Phil. degree in 2014 (and was awarded a commendation for his graduate thesis). As a graduate student he studied the reactivity of group 15 Zintl anions toward small molecules. His research included development of the chemistry of 1,2,3-tripnictolide anions. Following a short stint as an EPSRC Doctoral Prize awardee, he has since left chemistry to work as an accountant.



Jose M. Goicoechea carried out his undergraduate degree at the University of Zaragoza in his home country of Spain. He obtained his Ph.D. degree from the University of Bath under the supervision of Michael Whittlesey in 2003. That same year he moved to the United States as a postdoctoral researcher, where he worked with Professor Slavi Sevov (University of Notre Dame) on the solution-phase reactivity of anionic deltahedral Zintl ions. He was appointed to a University Lectureship in Inorganic Chemistry at the University of Oxford and to the fellowship of Lady Margaret Hall in 2006. In 2014 he was awarded an ACS Organometallics Young Investigator Fellowship and elected as a "Rising Star" at the 41st International Conference on Coordination Chemistry (ICCC). His research interests span organometallic synthesis and the chemistry of the main-group and transition-metal elements.

ACKNOWLEDGMENTS

This review encompasses over 120 years' worth of research on the solution-phase chemistry of group 15 Zintl cluster anions. We gratefully acknowledge the selfless dedication of the dozens of researchers who have contributed to this area. For our part, we would like to thank the EPSRC and the University of Oxford for financial support of this research (DTA studentship RSPT).

ABBREVIATIONS

12-crown-4	1,4,7,10-tetraoxacyclododecane
18-crown-6	1,4,7,10,13,16-hexaoxacyclooctadecane
2,2,2-crypt	4,7,13,16,21,24-hexaoxa-1,10-diazabicyclo[8.8.8]-hexacosane
Å	angstrom
Ad	1-adamantyl
av	average (mean)
Cp	cyclopentadienide
Cy	cyclohexyl
DFT	density functional theory
Dipp	2,6-diisopropylphenyl
DME	dimethoxyethane
DMF	N,N-dimethylformamide

en	ethylenediamine
ESR	electron spin resonance
Et	ethyl
Hex	hexyl
HOMO	highest occupied molecular orbital
Hz	hertz
<i>i</i> Pr	isopropyl
IR	infrared
<i>J</i>	coupling constant
kJ	kilojoule
MAS	magic angle spinning
Me	methyl
mes	mesityl
<i>n</i> Bu	<i>n</i> -butyl
NMR	nuclear magnetic resonance
Ph	phenyl
PMDETA	pentamethyldiethylenediamine
ppm	parts per million
<i>t</i> Bu	<i>tert</i> -butyl
THF	tetrahydrofuran
TMEDA	tetramethylethylenediamine

REFERENCES

- (1) Cossairt, B. M.; Piro, N. A.; Cummins, C. C. *Chem. Rev.* **2010**, *110*, 4164.
- (2) Caporali, M.; Gonsalvi, L.; Rossin, A.; Peruzzini, M. *Chem. Rev.* **2010**, *110*, 4178.
- (3) Scheer, M.; Balázs, G.; Seitz, A. *Chem. Rev.* **2010**, *110*, 4236.
- (4) Johnson, B. P.; Balázs, G.; Scheer, M. *Coord. Chem. Rev.* **2006**, *250*, 1178.
- (5) Figueroa, J. S.; Cummins, C. C. *Dalton Trans.* **2006**, 2161.
- (6) Peruzzini, M.; Gonsalvi, L.; Romerosa, A. *Chem. Soc. Rev.* **2005**, *34*, 1038.
- (7) Scherer, O. J. *Angew. Chem., Int. Ed. Engl.* **1990**, *29*, 1104.
- (8) Scherer, O. J. *Acc. Chem. Res.* **1999**, *32*, 751.
- (9) Dielmann, F.; Sierka, M.; Virovets, A. V.; Scheer, M. *Angew. Chem., Int. Ed.* **2010**, *49*, 6860.
- (10) Giffin, N. A.; Masuda, J. D. *Coord. Chem. Rev.* **2011**, *255*, 1342.
- (11) Scharfe, S.; Kraus, F.; Stegmaier, S.; Schier, A.; Fässler, T. F. *Angew. Chem., Int. Ed.* **2011**, *50*, 3630.
- (12) Fässler, T. F. *Struct. Bonding (Berlin)* **2011**, *140*, 91.
- (13) Joannis, A. C. R. *Hebd. Séances Acad. Sci.* **1891**, *113*, 795.
- (14) Joannis, A. C. R. *Hebd. Séances Acad. Sci.* **1892**, *114*, 585.
- (15) Joannis, A. *Ann. Chim. Phys.* **1906**, *7*, 5.
- (16) Kraus, C. A. *J. Am. Chem. Soc.* **1907**, *29*, 1557.
- (17) Smyth, F. H. *J. Am. Chem. Soc.* **1917**, *39*, 1299.
- (18) Peck, E. B. *J. Am. Chem. Soc.* **1918**, *40*, 335.
- (19) Zintl, E.; Harder, A. *Z. Phys. Chem., Abt. A* **1931**, *154*, 47.
- (20) Zintl, E.; Dullenkopf, W. *Z. Phys. Chem., Abt. B* **1932**, *16*, 183.
- (21) Zintl, E.; Goubeau, J.; Dullenkopf, W. *Z. Phys. Chem., Abt. A* **1931**, *154*, 1.
- (22) Zintl, E.; Kaiser, H. *Z. Anorg. Allg. Chem.* **1933**, *211*, 113.
- (23) Kummer, D.; Diehl, L. *Angew. Chem., Int. Ed. Engl.* **1970**, *9*, 895.
- (24) Corbett, J. D.; Adolphson, D. G.; Merryman, D. J.; Edwards, P. A.; Armatis, F. *J. Am. Chem. Soc.* **1975**, *97*, 6267.
- (25) Adolphson, D. G.; Corbett, J. D.; Merryman, D. J. *J. Am. Chem. Soc.* **1976**, *98*, 7234.
- (26) Corbett, J. D. *Chem. Rev.* **1985**, *85*, 383.
- (27) Corbett, J. D. *Angew. Chem., Int. Ed.* **2000**, *39*, 670.
- (28) Baudler, M. *Angew. Chem., Int. Ed. Engl.* **1982**, *21*, 492.
- (29) Baudler, M.; Glinka, K. *Chem. Rev.* **1993**, *93*, 1623.
- (30) Baudler, M. *Angew. Chem., Int. Ed. Engl.* **1987**, *26*, 419.
- (31) von Schnering, H. G.; Höhne, W. *Chem. Rev.* **1988**, *88*, 243.
- (32) Baudler, M.; Adamek, C.; Opiela, S.; Budzikiewicz, H.; Ouzounis, D. *Angew. Chem., Int. Ed. Engl.* **1988**, *27*, 1059.
- (33) Baudler, M.; Düster, D.; Germeshausen, J. *Z. Anorg. Allg. Chem.* **1986**, *534*, 19.

- (34) Gascoin, F.; Sevov, S. C. *J. Am. Chem. Soc.* **2000**, *122*, 10251.
 (35) Emmerling, F.; Röhr, C. Z. *Naturforsch.* **2002**, *57b*, 963.
 (36) Gascoin, F.; Sevov, S. C. *Inorg. Chem.* **2001**, *40*, 5177.
 (37) Emmerling, F.; Petri, D.; Röhr, C. Z. *Anorg. Allg. Chem.* **2004**, *630*, 2490.
 (38) Abicht, H.-P.; Höhle, W.; von Schnerring, H. G. Z. *Anorg. Allg. Chem.* **1984**, *519*, 7.
 (39) von Schnerring, H. G.; Meyer, T.; Höhle, W.; Schmettow, W.; Hinze, U.; Bauhofer, W.; Kliche, G. Z. *Anorg. Allg. Chem.* **1987**, *553*, 261.
 (40) Schmettow, W.; Lipka, A.; von Schnerring, H. G. *Angew. Chem., Int. Ed. Engl.* **1974**, *13*, 345.
 (41) Höhle, W.; Krogull, G.; Peters, K.; von Schnerring, H. Z. *Kristallogr.-New Cryst. Struct.* **1999**, *214*, 17.
 (42) Manriquez, V.; Höhle, W.; von Schnerring, H. G. Z. *Anorg. Allg. Chem.* **1986**, *539*, 95.
 (43) Santandrea, R. P.; Mensing, C.; von Schnerring, H. G. *Thermochim. Acta* **1986**, *98*, 301.
 (44) Meyer, T.; Höhle, W.; von Schnerring, H. G. Z. *Anorg. Allg. Chem.* **1987**, *552*, 69.
 (45) Dahlmann, W.; von Schnerring, H. G. *Naturwissenschaften* **1972**, *59*, 420.
 (46) Dahlmann, W.; von Schnerring, H. G. *Naturwissenschaften* **1973**, *60*, 429.
 (47) Höhle, W.; Buresch, J.; Peters, K.; Chang, J. H.; von Schnerring, H. Z. *Kristallogr.-New Cryst. Struct.* **2002**, *217*, 485.
 (48) Höhle, W.; Buresch, J.; Peters, K.; Chang, J. H.; von Schnerring, H. Z. *Kristallogr.-New Cryst. Struct.* **2002**, *217*, 487.
 (49) Höhle, W.; Buresch, J.; Wolf, J.; Peters, K.; Chang, J. H.; von Schnerring, H. Z. *Kristallogr.-New Cryst. Struct.* **2002**, *217*, 489.
 (50) Schmettow, W.; von Schnerring, H. G. *Angew. Chem., Int. Ed. Engl.* **1977**, *16*, 857.
 (51) Dorn, F. W.; Klemm, W. Z. *Anorg. Allg. Chem.* **1961**, *309*, 189.
 (52) Hirschle, C.; Röhr, C. Z. *Anorg. Allg. Chem.* **2000**, *626*, 1992.
 (53) Wichelhaus, W.; von Schnerring, H. G. *Naturwissenschaften* **1973**, *60*, 104.
 (54) von Schnerring, H. G.; Somer, M.; Kliche, G.; Höhle, W.; Meyer, T.; Wolf, J.; Ohse, L.; Kempa, P. B. Z. *Anorg. Allg. Chem.* **1991**, *601*, 13.
 (55) Emmerling, F.; Röhr, C. Z. *Anorg. Allg. Chem.* **2003**, *629*, 467.
 (56) Xu, L.; Bobev, S.; El-Bahraoui, J.; Sevov, S. C. *J. Am. Chem. Soc.* **2000**, *122*, 1838.
 (57) Kraus, F.; Aschenbrenner, J. C.; Korber, N. *Angew. Chem., Int. Ed.* **2003**, *42*, 4030.
 (58) Kraus, F.; Korber, N. *Chem.—Eur. J.* **2005**, *11*, 5945.
 (59) Kraus, F.; Korber, N. *Inorg. Chem.* **2006**, *45*, 1117.
 (60) Hanauer, T.; Kraus, F.; Reil, M.; Korber, N. *Monatsh. Chem.* **2006**, *137*, 147.
 (61) Critchlow, S. C.; Corbett, J. D. *Inorg. Chem.* **1984**, *23*, 770.
 (62) Cisar, A.; Corbett, J. D. *Inorg. Chem.* **1977**, *16*, 2482.
 (63) Kuznetsov, A. N.; Fässler, T. F. Z. *Anorg. Allg. Chem.* **2002**, *628*, 2537.
 (64) Benda, C. B.; Fässler, T. F. Z. *Anorg. Allg. Chem.* **2014**, *640*, 40.
 (65) Baudler, M.; Düster, D.; Ouzounis, D. Z. *Anorg. Allg. Chem.* **1987**, *544*, 87.
 (66) Baudler, M.; Akpapoglu, S.; Ouzounis, D.; Wasgestian, F.; Meinigke, B.; Budzikiewicz, H.; Münster, H. *Angew. Chem., Int. Ed. Engl.* **1988**, *27*, 280.
 (67) Milyukov, V. A.; Kataev, A. V.; Sinyashin, O. G.; Hey-Hawkins, E. *Russ. Chem. Bull. Int. Ed.* **2006**, *55*, 1297.
 (68) Korber, N.; Richter, F. *Angew. Chem., Int. Ed. Engl.* **1997**, *36*, 1512.
 (69) Kraus, F.; Hanauer, T.; Korber, N. *Angew. Chem., Int. Ed.* **2005**, *44*, 7200.
 (70) Höhle, W.; von Schnerring, H. G.; Schmidpeter, A.; Burget, G. *Angew. Chem., Int. Ed. Engl.* **1984**, *23*, 817.
 (71) Korber, N.; Daniels, J. *Helv. Chim. Acta* **1996**, *79*, 2083.
 (72) Korber, N.; Daniels, J. Z. *Anorg. Allg. Chem.* **1999**, *625*, 189.
 (73) Korber, N.; Daniels, J. *J. Chem. Soc., Dalton Trans.* **1996**, *1653*.
 (74) Korber, N.; Daniels, J. *Acta Crystallogr., Sect. C* **1996**, *52*, 2454.
 (75) Korber, N.; von Schnerring, H. G. *Chem. Ber.* **1996**, *129*, 155.
 (76) Bashall, A.; Beswick, M. A.; Choi, N.; Hopkins, A. D.; Kidd, S. J.; Lawson, Y. G.; Mosquera, M. E. G.; McPartlin, M.; Raithby, P. R.; Wheatley, A. E. H.; Wood, J. A.; Wright, D. S. *J. Chem. Soc., Dalton Trans.* **2000**, *479*.
 (77) Hanauer, T.; Grothe, M.; Reil, M.; Korber, N. *Helv. Chim. Acta* **2005**, *88*, 950.
 (78) Somer, M.; Höhle, W.; von Schnerring, H. G. Z. *Naturforsch.* **1989**, *44b*, 296.
 (79) Driess, M.; Merz, K.; Pritzkow, H.; Janoschek, R. *Angew. Chem., Int. Ed. Engl.* **1996**, *35*, 2507.
 (80) Hübler, K.; Becker, G. Z. *Anorg. Allg. Chem.* **1998**, *624*, 483.
 (81) Korber, N.; von Schnerring, H. G. Z. *Kristallogr.-New Cryst. Struct.* **1997**, *212*, 85.
 (82) Castleman, A. W.; Khanna, S. N.; Sen, A.; Reber, A. C.; Qian, M.; Davis, K. M.; Peppernick, S. J.; Ugrinov, A.; Merritt, M. D. *Nano Lett.* **2007**, *7*, 2734.
 (83) Beswick, M. A.; Choi, N.; Harmer, C. N.; Hopkins, A. D.; McPartlin, M.; Wright, D. S. *Science* **1998**, *281*, 1500.
 (84) Diehl, L.; Khodadadeh, K.; Kummer, D.; Strähle, J. Z. *Naturforsch.* **1976**, *31b*, 522.
 (85) Breunig, H. J.; Ghesner, M. E.; Lork, E. Z. *Anorg. Allg. Chem.* **2005**, *631*, 851.
 (86) Mutzbauer, F.; Korber, N. *Acta Crystallogr., Sect. E* **2011**, *67*, m1551.
 (87) Reil, M.; Korber, N. Z. *Anorg. Allg. Chem.* **2007**, *633*, 1599.
 (88) Korber, N.; Daniels, J.; von Schnerring, H. G. *Angew. Chem., Int. Ed. Engl.* **1996**, *35*, 1107.
 (89) Knettel, D.; Reil, M.; Korber, N. Z. *Naturforsch.* **2001**, *56b*, 965.
 (90) Korber, N.; Daniels, J. Z. *Anorg. Allg. Chem.* **1996**, *622*, 1833.
 (91) Korber, N.; Daniels, J. *Polyhedron* **1996**, *15*, 2681.
 (92) Dai, F. R.; Xu, L. *Chin. J. Struct. Chem.* **2007**, *26*, 45.
 (93) Belin, C. H. E. *J. Am. Chem. Soc.* **1980**, *102*, 6036.
 (94) Bolle, U.; Tremel, W. *J. Chem. Soc., Chem. Commun.* **1992**, *91*.
 (95) Jun, Z.; Li, X. U. *Chin. J. Struct. Chem.* **2011**, *30*, 1091.
 (96) Garcia, F.; Less, R. J.; Naseri, V.; McPartlin, M.; Rawson, J. M.; Tomas, M. S.; Wright, D. S. *Chem. Commun.* **2008**, 859.
 (97) Weinert, B.; Eulenstein, A. R.; Ababei, R.; Dehnen, S. *Angew. Chem., Int. Ed.* **2014**, *53*, 4704.
 (98) Miluykov, V.; Kataev, A.; Sinyashin, O.; Lönncke, P.; Hey-Hawkins, E. Z. *Anorg. Allg. Chem.* **2006**, *632*, 1728.
 (99) Hanauer, T.; Aschenbrenner, J. C.; Korber, N. *Inorg. Chem.* **2006**, *45*, 6723.
 (100) Baudler, M.; Düster, D. Z. *Naturforsch.* **1987**, *42b*, 335.
 (101) von Schnerring, H. G.; Manriquez, V.; Höhle, W. *Angew. Chem., Int. Ed. Engl.* **1981**, *20*, 594.
 (102) Baudler, M.; Düster, D.; Langerbeins, K.; Germeshausen, J. *Angew. Chem., Int. Ed. Engl.* **1984**, *23*, 317.
 (103) Korber, N. *Phosphorus Sulfur Silicon Relat. Elem.* **1997**, *124*, 339.
 (104) Haushalter, R. C.; Eichhorn, B. W.; Rheingold, A. L.; Geib, S. J. *J. Chem. Soc., Chem. Commun.* **1988**, 1027.
 (105) Baudler, M.; Heumüller, R.; Düster, D.; Germeshausen, J.; Hahn, J. Z. *Anorg. Allg. Chem.* **1984**, *518*, 7.
 (106) Baudler, M.; Exner, O. *Chem. Ber.* **1983**, *116*, 1268.
 (107) Baudler, M.; Heumüller, R.; Hahn, J. Z. *Anorg. Allg. Chem.* **1985**, *529*, 7.
 (108) Guérin, F.; Richeson, D. *Inorg. Chem.* **1995**, *34*, 2793.
 (109) Mandal, S.; Liu, R.; Reber, A. C.; Qian, M.; Saavedra, H. M.; Ke, X.; Schiffer, P.; Sen, S.; Weiss, P. S.; Khanna, S. N.; Sen, A. *Chem. Commun.* **2011**, *47*, 3126.
 (110) Höhle, W.; von Schnerring, H. G. *Angew. Chem., Int. Ed. Engl.* **1986**, *25*, 352.
 (111) Baudler, M.; Glinka, K.; Jones, R. A. *Inorg. Synth.* **1990**, *27*, 227.
 (112) Schmidbauer, H.; Bauer, A. *Phosphorus Sulfur Silicon Relat. Elem.* **1995**, *102*, 217.

- (113) Hendriksen, C. J. H. Alkoxide Packaged Sodium Dihydrogenphosphide: Synthesis and Reactivity, Ph.D. thesis, ETH Zurich, nr. 20148, 2012.
- (114) Greenwood, N. N.; Earnshaw, A. *Chemistry of the Elements*, 2nd ed.; Butterworth Heinemann: Oxford, 1997.
- (115) Simon, A.; Borrmann, H.; Craubner, H. *Phosphorus Sulfur Silicon Relat. Elem.* **1987**, *30*, 507.
- (116) Sen, T.; Poupko, R.; Fleischer, U.; Zimmermann, H.; Luz, Z. *J. Am. Chem. Soc.* **2000**, *122*, 889.
- (117) Seifert, G.; Jones, R. O. *J. Chem. Phys.* **1992**, *96*, 2951.
- (118) Schröder, G. *Angew. Chem., Int. Ed. Engl.* **1963**, *2*, 481.
- (119) Oth, J. F. M.; Müllen, K.; Gilles, J.-M.; Schröder, G. *Helv. Chim. Acta* **1974**, *57*, 1415.
- (120) Poupko, R.; Zimmermann, H.; Müller, K.; Luz, Z. *J. Am. Chem. Soc.* **1996**, *118*, 7995.
- (121) Baudler, M.; Heumüller, R.; Langerbeins, K. *Z. Anorg. Allg. Chem.* **1984**, *S14*, 7.
- (122) Aschenbrenner, J. C.; Korber, N. *Z. Anorg. Allg. Chem.* **2004**, *630*, 31.
- (123) Dai, F.-R.; Xu, L. *Inorg. Chim. Acta* **2006**, *359*, 4265.
- (124) Turberville, R. S. P.; Goicoechea, J. M. *Organometallics* **2012**, *31*, 2452.
- (125) Turberville, R. S. P.; Goicoechea, J. M. *Eur. J. Inorg. Chem.* **2014**, 1660.
- (126) Korber, N.; von Schnering, H. G. *J. Chem. Soc., Chem. Commun.* **1995**, 1713.
- (127) Baudler, M.; Ternberger, H.; Faber, W.; Hahn, J. *Z. Naturforsch.* **1979**, *34b*, 1690.
- (128) Baudler, M.; Riekehof-Böhner, R. *Z. Naturforsch.* **1985**, *40b*, 1424.
- (129) Fritz, G.; Biastoch, R.; Stoll, K.; Vaahs, T.; Hanke, D.; Schneider, H. W. *Phosphorus Sulfur Silicon Relat. Elem.* **1987**, *30*, 385.
- (130) Fritz, G.; Härrer, J.; Matern, E. *Z. Anorg. Allg. Chem.* **1983**, *504*, 38.
- (131) Noblet, P.; Cappello, V.; Tekautz, G.; Baumgartner, J.; Hassler, K. *Eur. J. Inorg. Chem.* **2011**, 101.
- (132) Charles, S.; Fettinger, J. C.; Eichhorn, B. W. *J. Am. Chem. Soc.* **1995**, *117*, 5303.
- (133) Mattamana, S. P.; Promprai, K.; Fettinger, J. C.; Eichhorn, B. W. *Inorg. Chem.* **1998**, *37*, 6222.
- (134) Milyukov, V. A.; Kataev, A. V.; Hey-Hawkins, E.; Sinyashin, O. *G. Russ. Chem. Bull., Int. Ed.* **2007**, *56*, 298.
- (135) Baudler, M.; Faber, W.; Hahn, J. *Z. Anorg. Allg. Chem.* **1980**, *469*, 15.
- (136) Fritz, G.; Hoppe, K. D.; Höhne, W.; Weber, D.; Mujica, C.; Manriquez, V.; von Schnering, H. G. *J. Organomet. Chem.* **1983**, *249*, 63.
- (137) Fritz, G.; Schneider, H.-W. *Z. Anorg. Allg. Chem.* **1990**, *584*, 12.
- (138) von Schnering, H. G.; Fenske, D.; Höhne, W.; Binnewies, M.; Peters, K. *Angew. Chem., Int. Ed. Engl.* **1979**, *18*, 679.
- (139) Fritz, G.; Layher, E.; Goesmann, H.; Hanke, D.; Persau, C. Z. *Anorg. Allg. Chem.* **1991**, *594*, 36.
- (140) Ahlrichs, R.; Fenske, D.; Fromm, K.; Krautscheid, H.; Krautscheid, U.; Treutler, O. *Chem.—Eur. J.* **1996**, *2*, 238.
- (141) Höhne, W.; von Schnering, H. G. *Z. Anorg. Allg. Chem.* **1978**, *440*, 171.
- (142) Turberville, R. S. P.; Goicoechea, J. M. *Chem. Commun.* **2012**, *48*, 1470.
- (143) Mansfield, N. E.; Grundy, J.; Coles, M. P.; Avent, A. G.; Hitchcock, P. B. *J. Am. Chem. Soc.* **2006**, *128*, 13879.
- (144) Knapp, C.; Zhou, B.; Denning, M. S.; Rees, N. H.; Goicoechea, J. M. *Dalton Trans.* **2010**, *39*, 426.
- (145) Qian, M.; Reber, A. C.; Ugrinov, A.; Chaki, N. K.; Mandal, S.; Saavedra, H. M.; Khanna, S. N.; Sen, A.; Weiss, P. S. *ACS Nano* **2010**, *4*, 235.
- (146) Mandal, S.; Reber, A. C.; Qian, M.; Liu, R.; Saavedra, H. M.; Sen, S.; Weiss, P. S.; Khanna, S. N.; Sen, A. *Dalton Trans.* **2012**, *41*, 12365.
- (147) Mandal, S.; Reber, A. C.; Qian, M.; Liu, R.; Saavedra, H. M.; Sen, S.; Weiss, P. S.; Khanna, S. N.; Sen, A. *Dalton Trans.* **2012**, *41*, 5454.
- (148) Knapp, C. M.; Large, J. S.; Rees, N. H.; Goicoechea, J. M. *Dalton Trans.* **2011**, *40*, 735.
- (149) Cossairt, B. M.; Cummins, C. C. *Angew. Chem., Int. Ed.* **2008**, *47*, 169.
- (150) Knapp, C. M. Solution Reactivity Studies of Group 15 Zintl Ions, D.Phil. thesis, University of Oxford, 2013.
- (151) Charles, S.; Fettinger, J. C.; Bott, S. G.; Eichhorn, B. W. *J. Am. Chem. Soc.* **1996**, *118*, 4713.
- (152) Kesanli, B.; Charles, S.; Lam, Y.-F.; Bott, S. G.; Fettinger, J.; Eichhorn, B. *J. Am. Chem. Soc.* **2000**, *122*, 11101.
- (153) Knapp, C. M.; Jackson, C. S.; Large, J. S.; Thompson, A. L.; Goicoechea, J. M. *Inorg. Chem.* **2011**, *50*, 4021.
- (154) Chaki, N. K.; Mandal, S.; Reber, A. C.; Qian, M.; Saavedra, H. M.; Weiss, P. S.; Khanna, S. N.; Sen, A. *ACS Nano* **2010**, *4*, 5813.
- (155) Moses, M. J.; Fettinger, J.; Eichhorn, B. *J. Am. Chem. Soc.* **2002**, *124*, 5944.
- (156) Eichhorn, B. W.; Haushalter, R. C.; Huffman, J. C. *Angew. Chem., Int. Ed. Engl.* **1989**, *28*, 1032.
- (157) Charles, S.; Eichhorn, B. W.; Rheingold, A. L.; Bott, S. G. *J. Am. Chem. Soc.* **1994**, *116*, 8077.
- (158) Bolle, U.; Tremel, W. *J. Chem. Soc., Chem. Commun.* **1994**, 217.
- (159) Charles, S.; Danis, J. A.; Mattamana, S. P.; Fettinger, J. C.; Eichhorn, B. W. *Z. Anorg. Allg. Chem.* **1998**, *624*, 823.
- (160) Charles, S.; Danis, J. A.; Fettinger, J. C.; Eichhorn, B. W. *Inorg. Chem.* **1997**, *36*, 3772.
- (161) Kesanli, B.; Mattamana, S. P.; Danis, J.; Eichhorn, B. *Inorg. Chim. Acta* **2005**, *358*, 3145.
- (162) Charles, S.; Fettinger, J. C.; Eichhorn, B. W. *Inorg. Chem.* **1996**, *35*, 1540.
- (163) Knapp, C. M.; Large, J. S.; Rees, N. H.; Goicoechea, J. M. *Chem. Commun.* **2011**, *47*, 4111.
- (164) Critchlow, S. C.; Corbett, J. D. *Inorg. Chem.* **1982**, *21*, 3286.
- (165) Xu, L.; Sevov, S. C. *Inorg. Chem.* **2000**, *39*, 5383.
- (166) Ababei, R.; Heine, J.; Holyńska, M.; Thiele, G.; Weinert, B.; Xie, X.; Weigend, F.; Dehnen, S. *Chem. Commun.* **2012**, *48*, 11295.
- (167) Xu, L.; Ugrinov, A.; Sevov, S. C. *J. Am. Chem. Soc.* **2001**, *123*, 4091.
- (168) Goicoechea, J. M.; Sevov, S. C. *Angew. Chem., Int. Ed.* **2006**, *45*, 5147.
- (169) Goicoechea, J. M.; Hull, M. W.; Sevov, S. C. *J. Am. Chem. Soc.* **2007**, *129*, 7885.
- (170) Lips, F.; Dehnen, S. *Angew. Chem., Int. Ed.* **2009**, *48*, 6435.
- (171) Lips, F.; Dehnen, S. *Angew. Chem., Int. Ed.* **2011**, *50*, 955.
- (172) Lips, F.; Clérac, R.; Dehnen, S. *Angew. Chem., Int. Ed.* **2011**, *50*, 960.
- (173) Lips, F.; Clérac, R.; Dehnen, S. *J. Am. Chem. Soc.* **2011**, *133*, 14168.
- (174) Lips, F.; Schellenberg, I.; Pöttgen, R.; Dehnen, S. *Chem.—Eur. J.* **2009**, *15*, 12968.
- (175) Lips, F.; Holyńska, M.; Clérac, R.; Linne, U.; Schellenberg, I.; Pöttgen, R.; Weigend, F.; Dehnen, S. *J. Am. Chem. Soc.* **2012**, *134*, 1181.
- (176) Weinert, B.; Weigend, F.; Dehnen, S. *Chem.—Eur. J.* **2012**, *18*, 13589.
- (177) Ababei, R.; Massa, W.; Harms, K.; Xie, X.; Weigend, F.; Dehnen, S. *Angew. Chem., Int. Ed.* **2013**, *52*, 13544.
- (178) von Schnering, H. G.; Wolf, J.; Weber, D.; Ramirez, R.; Meyer, T. *Angew. Chem., Int. Ed. Engl.* **1986**, *25*, 353.
- (179) Eichhorn, B. W.; Mattamana, S. P.; Gardner, D. R.; Fettinger, J. C. *J. Am. Chem. Soc.* **1998**, *120*, 9708.
- (180) Kesanli, B.; Fettinger, J.; Eichhorn, B. *J. Am. Chem. Soc.* **2003**, *125*, 7367.
- (181) Kesanli, B.; Fettinger, J.; Scott, B.; Eichhorn, B. *Inorg. Chem.* **2004**, *43*, 3840.
- (182) Li, J.; Wu, K. *Inorg. Chem.* **2000**, *39*, 1538.

- (183) Moses, M. J.; Fettinger, J. C.; Eichhorn, B. W. *Science* **2003**, *300*, 778.
- (184) Moses, M. J.; Fettinger, J. C.; Eichhorn, B. W. *Inorg. Chem.* **2007**, *46*, 1036.
- (185) Tran, N. T.; Powell, D. R.; Dahl, L. F. *Angew. Chem., Int. Ed.* **2000**, *39*, 4121.
- (186) Charles, S.; Eichhorn, B. W.; Bott, S. G. *J. Am. Chem. Soc.* **1993**, *115*, 5837.
- (187) Wade, K. *J. Chem. Soc. D* **1971**, 792.
- (188) Wade, K. *Adv. Inorg. Chem. Radiochem.* **1976**, *18*, 1.
- (189) Mingos, D. M. P. *Nat. Phys. Sci.* **1972**, *236*, 99.
- (190) Mingos, D. M. P. *Acc. Chem. Res.* **1984**, *17*, 311.
- (191) von Hänisch, C.; Fenske, D.; Weigend, F.; Ahlrichs, R. *Chem.—Eur. J.* **1997**, *3*, 1494.
- (192) von Hänisch, C.; Fenske, D. *Z. Anorg. Allg. Chem.* **1998**, *624*, 367.
- (193) Knapp, C. M.; Westcott, B. H.; Raybould, M. A. C.; McGrady, J. E.; Goicoechea, J. M. *Angew. Chem., Int. Ed.* **2012**, *51*, 9097.
- (194) Knapp, C. M.; Westcott, B. H.; Raybould, M. A. C.; McGrady, J. E.; Goicoechea, J. M. *Chem. Commun.* **2012**, *48*, 12183.
- (195) Dillon, K. B.; Mathey, F.; Nixon, J. F. *Phosphorus: the Carbon Copy: From Organophosphorus to Phospha-organic Chemistry*; Wiley: Chichester, 1998.
- (196) Mathey, F. *Angew. Chem., Int. Ed.* **2003**, *42*, 1578.
- (197) Turberville, R. S. P.; Goicoechea, J. M. *Chem. Commun.* **2012**, *48*, 6100.
- (198) Turberville, R. S. P.; Jupp, A. R.; McCullough, P. S. B.; Ergömen, D.; Goicoechea, J. M. *Organometallics* **2013**, *32*, 2234.
- (199) Turberville, R. S. P.; Goicoechea, J. M. *Inorg. Chem.* **2013**, *52*, 5527.
- (200) Turberville, R. S. P. Solution Reactivity Studies of Group 15 Zintl Ions Towards Unsaturated Substrates, D.Phil. thesis, University of Oxford, 2014.
- (201) Baudler, M.; Hahn, J. *Z. Naturforsch.* **1990**, *45b*, 1139.
- (202) Maigrot, N.; Sierra, M.; Charrier, C.; Mathey, F. *Bull. Soc. Chim. Fr.* **1994**, *131*, 397.
- (203) Butts, C. P.; Green, M.; Hooper, T. N.; Kilby, R. J.; McGrady, J. E.; Pantazis, D. A.; Russell, C. A. *Chem. Commun.* **2008**, 856.
- (204) Scherer, O. J.; Hilt, T.; Wolmershäuser, G. *Angew. Chem., Int. Ed.* **2000**, *39*, 1425.
- (205) Deng, S.; Schwarzmaier, C.; Eichhorn, C.; Scherer, O.; Wolmershäuser, G.; Zabel, M.; Scheer, M. *Chem. Commun.* **2008**, 4064.
- (206) Kolb, H. C.; Finn, M. G.; Sharpless, K. B. *Angew. Chem., Int. Ed. Engl.* **2001**, *40*, 2004.
- (207) Jupp, A. R.; Goicoechea, J. M. *Angew. Chem., Int. Ed.* **2013**, *52*, 10064.
- (208) Becker, G.; Schwarz, W.; Seidler, N.; Westerhausen, M. *Z. Anorg. Allg. Chem.* **1992**, *612*, 72.
- (209) Puschmann, F. F.; Stein, D.; Heift, D.; Hendriksen, C.; Gal, Z. A.; Grütmacher, H.-F.; Grütmacher, H. *Angew. Chem., Int. Ed.* **2011**, *50*, 8420.
- (210) Heift, D.; Benkő, Z.; Grütmacher, H. *Dalton Trans.* **2014**, *43*, 831.
- (211) Lu, Y.; Wang, H.; Xie, Y.; Liu, H.; Schaefer, H. F. *Inorg. Chem.* **2014**, *53*, 6252.
- (212) Heift, D.; Benkő, Z.; Grütmacher, H. *Dalton Trans.* **2014**, *43*, 5920.
- (213) Chen, X.; Alidori, S.; Puschmann, F. F.; Santiso-Quinones, G.; Benkő, Z.; Li, Z.; Becker, G.; Grütmacher, H.-F.; Grütmacher, H. *Angew. Chem., Int. Ed.* **2014**, *53*, 1641.
- (214) Heift, D.; Benkő, Z.; Grütmacher, H. *Angew. Chem., Int. Ed.* **2014**, *53*, 6757.
- (215) Alidori, S.; Heift, D.; Santiso-Quinones, G.; Benkő, Z.; Grütmacher, H.; Caporali, M.; Gonsalvi, L.; Rossin, A.; Peruzzini, M. *Chem.—Eur. J.* **2012**, *18*, 14805.
- (216) Jupp, A. R.; Goicoechea, J. M. *J. Am. Chem. Soc.* **2013**, *135*, 19131.
- (217) During the copy editing of this review article the first example of the $[\text{Bi}_7]^{3-}$ trianion was reported by Sesov and co-workers: Perla, L. G.; Oliver, A. G.; Sesov, S. C. *Inorg. Chem.* **2014**, DOI: 10.1021/ic502158e.